THESIS

EFFECTS OF WHITEWATER PARKS ON FISH PASSAGE:

A SPATIALLY EXPLICIT HYDRAULIC ANALYSIS

Submitted by

Timothy A. Stephens

Department of Civil and Environmental Engineering

In partial fulfillment of the requirements

For the Degree of Master of Science

Colorado State University

Fort Collins, Colorado

Fall 2014

Master's Committee:

Advisor: Brian P. Bledsoe

Christopher A. Myrick
Peter A. Nelson

ABSTRACT

EFFECTS OF WHITEWATER PARKS ON FISH PASSAGE: A SPATIALLY EXPLICIT HYDRAULIC ANALYSIS

Whitewater parks (WWPs) provide a valuable recreational and economic resource that is rapidly growing in popularity throughout the United States. WWPs were originally thought to enhance aquatic habitat; however, recent studies have shown that the hydraulic conditions required to meet recreational needs can act as a partial barrier to upstream migrating trout and that WWP pools may contain lower densities of fish compared to natural pools. There is limited knowledge of the direct effects of WWPs on fish passage. Managers and policy makers are forced to review WWP designs and make permit decisions without sound scientific evidence. It is also difficult to make design recommendations for future WWPs and possibly retrofitting existing WWPs to allow for successful fish passage without improved understanding of the factors contributing to suppression of movement in WWPs. We describe novel approaches combining fish movement data and hydraulic results from a three-dimensional computational fluid dynamics model to examine the physical processes that limit upstream movement of trout in an actual WWP in Lyons, Colorado. These methods provide a continuous and spatially explicit description of velocity, depth, vorticity, and turbulent kinetic energy (TKE) along potential fish swimming paths in the flow field. Variation in the magnitude and distribution of velocity and depth relative to fish swimming ability is reflective of variation in passage success among WWP structures and size classes of fish. Logistic regression analyses indicate a significant influence of velocity and depth on limiting passage success and accurately predict > 86 percent observed fish movements. Relationships emerge at individual WWP structures that

highlight unique hydraulic characteristics and their effect on passage success. The methods described in this study provide a powerful approach to quantify hydraulic conditions at a scale meaningful to a fish and mechanistically evaluate the effects of hydraulic structures on fish passage. The results of these analyses can be used for management and design guidance, have implications for fishes with lesser swimming abilities, and demonstrate the need to assess additional WWPs of various sizes.

ACKNOWLEDGMENTS

It has been a wonderful experience and opportunity to learn in such an enabling environment as Colorado State. I would like to thank my advisor, Brian Bledsoe, for his advice and guidance throughout the entirety of this research and my graduate degree. I would also like to thank Chris Myrick and Peter Nelson for their advice as committee members; the Colorado Water Conservation Board (CWCB) and the Colorado Water Institute (CWI) for funding support; Brian Fox and Nell Kolden; Matt Kondratieff at Colorado Parks and Wildlife (CPW); my friends and family for their support; and countless others who have aided me in guidance or support along the way.

TABLE OF CONTENTS

LIST OF TABLES

LIST OF FIGURES

LIST OF SYMBOLS

Symbols

d	distance between two nodes
$\hat{i}, \hat{j}, \hat{k}$	unit vector in the *x*, *y*, and *z* directions, respectively
rms	root-mean-square
u, v, w	*x*, *y*, and *z* components of velocity, respectively
v	velocity
v_{burst}	burst swimming ability
v_{rms}	average *rms* velocity between two nodes
v_x, v_y, v_z	velocity in the *x*-plane, *y*-plane, *z*-plane orientation, respectively
x, *y*, *z*	planes with a directional component relative to the *x*-direction
σ	standard deviation
$\bar{\xi}$	3-D vorticity

Statistical Terms

df	degrees of freedom
e^{β}	odds ratio
p	p value
SE	standard error
β	beta
χ^2	significance was evaluated using the chi-square statistic

UNITS OF MEASURE

BL	body length(s)
BL/s	body length(s) per second
cfs	cubic feet per second
ft	feet
ft/s	feet per second
ft^2	square feet
ft^2/s^2	square feet per square second
ft^3/s^2	cubic feet per square second
%	percent
mi	mile(s)
mm	millimeter(s)
s^{-1}	frequency

CHAPTER 1 INTRODUCTION

1.1 Whitewater Parks and Water Resources

Riverine biota have evolved to inhabit highly complex hydraulic environments formed through natural hydrologic variability and geomorphic response (Poff *et al*., 1997; Nestler *et al*., 2012; Thorp *et al*., 2006). Aquatic organisms exploit habitats that vary spatially and temporally across dimensions and scales, thus highlighting the need for connectivity of the river landscape (Fausch *et al*., 2002; Frissel *et al*., 1986). For example, many fishes migrate in search of optimal habitats for spawning, rearing, overwintering, and other life-cycle processes (Schlosser and Angermeier, 1995). The reproductive success of migratory fishes and other organisms is dependent on the quantity, quality, and connectivity of available habitats from large-scale systems as they vary slowly and are disrupted infrequently, down to smaller habitat patches that are disturbed and change more frequently (Frissel *et al*., 2001).

Anthropogenic needs require the exploitation of water resources resulting in fragmentation of many rivers by dams, diversions, and other in-stream structures. When impassable, these structures cut-off necessary habitat linkages and migration routes of aquatic organisms, particularly fishes (Dudley and Platania, 2007; Fullerton *et al*., 2010; Walters *et al*., 2014). There is a strong interdependence among organisms within an ecosystem, and the extirpation of a species could alter the entire ecosystem energy flow and composition (Baxter *et al*., 2004). Successful passage for fishes of all life stages across barriers to migration is imperative to restore and maintain ecosystem function (Beechie *et al*., 2010; Bunt *et al*., 2012; Wohl *et al*., 2005). In-stream structures must operate within the physiological limits of a fish's swimming abilities, and understanding how fish respond to micro-hydrodynamic and macro-

hydrodynamic conditions within a structure is necessary to effectively design for passage success (Williams *et al*., 2012).

However, structures are designed and constructed without direct knowledge of fish passage success in response to altered hydraulic conditions. A whitewater park (WWP) consists of one or more in-stream structures primarily constructed to create a hydraulic jump that is desirable to recreational kayakers and other boaters. The hydraulic jump is typically formed by grouting a laterally constricted chute over a steep drop into a downstream pool. WWPs provide a valuable recreational and economic resource (Hagenstad *et al*., 2000) that is rapidly growing in popularity throughout communities in the United States, with Colorado being an epicenter of WWP design and construction (Fox, 2013). Currently there are 22 constructed and 12 proposed WWPs in the state of Colorado (Kondratieff, pers. comm.). WWPs were originally thought to enhance aquatic habitat (McGrath, 2003); however, recent studies (Fox, 2013; Kolden, 2013) have shown that WWPs can act as a partial barrier to upstream migrating trout, and WWP pools may contain lower densities of fish compared to natural pools. Further, the magnitude of suppressed fish movement varies at different WWP structures and among size classes of fish. Higher velocities with larger spatial distributions were recorded in WWPs compared to natural reaches, and unique hydraulic conditions exist at individual WWP structures as a result of seemingly subtle differences in their design and configuration. Concerns have arisen that the hydraulic conditions required to meet recreational needs are contributing to the suppression of movement of upstream migrating fishes, thereby disrupting the longitudinal connectivity of a river.

1.2 Fish Swimming Abilities

Fish exhibit multiple modes of swimming when encountering different flow velocities in order to maximize ground speed and minimize energy expenditure (Beamish, 1978; Katopodis, 2005). Additionally, the swimming ability of fishes is directly related to fish body length (BL) (Beamish, 1978; Castro-Santos *et al*., 2013; Peake *et al*., 1997; Webb, 1998). Velocity can act as a burst swimming barrier in which the velocity of the water is greater than the fish's maximum swim speed. Velocity can also act as an exhaustive swimming barrier where a fish is unable to maintain positive ground speed over the required distance. Previous laboratory studies have observed burst swimming abilities of 10 to 15 BL/s (Beamish, 1978; Peake *et al*., 1997); however, a more recent study observed burst swimming abilities of brook trout (*Salvelinus fontinalis*) and brown trout (*Salmo trutta*) of up to 25 BL/s (Castro-Santos *et al*., 2013).

Adequate depth is required for a fish to reach its full swimming potential (Webb, 1975). Minimum flow depths in a WWP are often located in zones of supercritical flow where velocities are greatest. Insufficient depth to submerge a fish impairs its ability to generate thrust through body and tail movements, exposes the gills limiting oxygen consumption, and exposes the fish to physical trauma through contact with the channel bed (Dane, 1978). Minimum depth recommendations for fish passage through culverts vary from 1.5 to 2.5 times the body depth of a fish depending on the species of interest, life stage, and regulating agency (Hotchkiss and Frei, 2007). For non-anadromous salmonids, typical depth recommendations range from 0.4 to 0.8 ft (Fitch, 1995; Hotchkiss and Frei, 2007; Kilgore *et al*., 2010; National Oceanic and Atmospheric Administration (NOAA), 2001).

Current knowledge of turbulence and its effects on fish swimming abilities suggests that turbulence might be contributing to the suppression of movement in WWPs. In particular,

vorticity and turbulent kinetic energy (TKE) are recognized as meaningful measures of turbulence (Lacey *et al*., 2012), and higher magnitudes of vorticity and TKE were observed in WWP pools compared to natural pools (Kolden, 2013). Numerous studies have investigated the effects of turbulence metrics such as TKE, turbulent intensity (TI), Reynolds' shear stress, and vorticity on fish swimming abilities. Turbulence can increase or decrease a fish's swimming ability (Cotel and Webb, 2012; Lacey *et al*., 2012; Liao, 2007); however, high levels of turbulence pose a stability challenge to fish (Tritico and Cotel, 2010), and turbulence reduces fish's swimming abilities at high current speeds (Lupandin, 2005; Pavlov *et al*., 2000). Fish migrating upstream through an experimental pool-type fishway appear to prefer locations of lower turbulence and velocity (Silva *et al*., 2012).

Despite current knowledge of fish passage and hydraulics, there is little understanding of the factors contributing to the suppression of fish movements in WWPs. Previous attempts to directly correlate fish passage with hydraulic variables yielded only poor predictors of passage success (Castro-Santos *et al*., 2009). Studies examining the effects of hydraulics on fish passage are limited by scale. Fish experience hydraulic conditions locally (Eulerian frame) and continuously along a movement path (Lagrangian frame) in a highly complex hydraulic environment (Goodwin *et al*., 2006). Studies employing Particle Image Velocimetry have the capability of quantifying hydraulics continuously along fish movement paths; however, the majority of these studies are limited to laboratory settings that constrain the transferability of results to natural environments (Cotel and Webb, 2012). Additional studies are limited to three-dimensional (3-D) point measurements or averaging over larger spatial scales that do not capture the continuous small-scale hydraulic heterogeneity important to a fish (Crowder and Diplas, 2000, 2006).

Consequently, the factors contributing the suppression of movement of upstream migrating fish in WWPs have not been mechanistically explained. Managers and policy makers are forced to make decisions and review designs regarding WWPs without sound scientific evidence. This problem has the potential to impose negative environmental impacts if a WWP that greatly disrupts the longitudinal connectivity of a river is approved. Alternatively, if a WWP does not pose a threat to the environment and is disapproved, a valuable recreational and economic opportunity will be missed. Without a direct understanding of the factors contributing to suppression of movement in WWPs, making informed management and policy decisions regarding WWPs will continue to be difficult and could have unintended consequences.

In order to determine the effect of hydraulic conditions on passage success, detailed fish movement data must be assessed in conjunction with hydraulic characteristics at a scale meaningful to a fish (Williams *et al*., 2012). Advancements in quantifying fish movement through passive integrated transponders (PIT) tags have increased our ability to monitor and evaluate passage success. Additionally, computational fluid dynamics (CFD) models provide a powerful means of estimating the fine-scale hydrodynamic conditions through which fish pass.

1.3 Objectives

We describe novel approaches combining fish movement data and hydraulic results from a 3-D computational fluid dynamics model to examine the physical processes that limit upstream movement of trout in an actual WWP in Lyons, Colorado. The objectives of this study are as follows:

1. Use the results from a 3-D CFD model to provide a continuous and spatially explicit description of velocity, depth, vorticity, and TKE along the flow field.

2. Compare the magnitudes and distribution of velocity, depth, vorticity, and TKE among three unique WWP structures on the St. Vrain River, Colorado, USA.
3. Determine the relationship between velocity, depth, vorticity, and TKE on the suppression of movement of upstream migrating fishes through statistical analysis of movement data from PIT-tag studies at the St. Vrain WWP.
4. Provide design recommendations and physically-based relationships that help managers better accommodate fish passage through WWP structures.

CHAPTER 2 METHODS

2.1 Study Site

Fish movement data and the results from a 3-D CFD model were available at a WWP located on the North Fork of the St. Vrain River in Lyons, Colorado (Fox, 2013; Kolden, 2013). The North Fork of the St. Vrain River originates on the east slope of the Rocky Mountains where it flows east to the foothills region in the town of Lyons and its confluence with the South Fork of the St. Vrain River. The study site consists of nine WWP structures along a 1,300-ft reach in Meadow Park. The natural river morphology at the study site can be described as the transition zone between a step-pool channel and a meandering pool-riffle channel. The natural river channel is characterized by riffles, runs, and shallow pools with cobble and boulder substrates. The North Fork of the St. Vrain River experiences a typical snowmelt hydrologic regime with peak flows occurring in late May to early June. Accurate U. S. Geological Survey (USGS) gage data were unavailable for the site due to a reservoir located approximately 8 mi upstream; however, a stage-discharge rating relationship was developed over the course of the study to provide a continuous record of discharges for the site (Fox, 2013).

2.2 Fish Movement Data and Hydraulic Modeling Results

2.2.1 Fish Movement Data

Fish passage was assessed at three WWP structures by obtaining 14 months of fish movement data from PIT-antenna arrays (Fox, 2013). Tagged salmonids, rainbow trout (*Oncorhynchus mykiss* and *Hofer x Harrison* strain) and brown trout (*Salmo trutta*), were included in the analysis totaling 536 tagged fishes ranging in size from 115 to 435 mm. Due to safety risks involving park users, PIT antennas were installed directly upstream of the WWP

structures and in the tail-out of the pools directly downstream of the WWP structures (Figure 2.1). The PIT-antenna configuration associated a time stamp and river discharge with a successful movement, but it did not provide information on failed attempts of individual fish. Therefore, fish were classified as fish that did pass a structure versus fish that did not pass a structure.

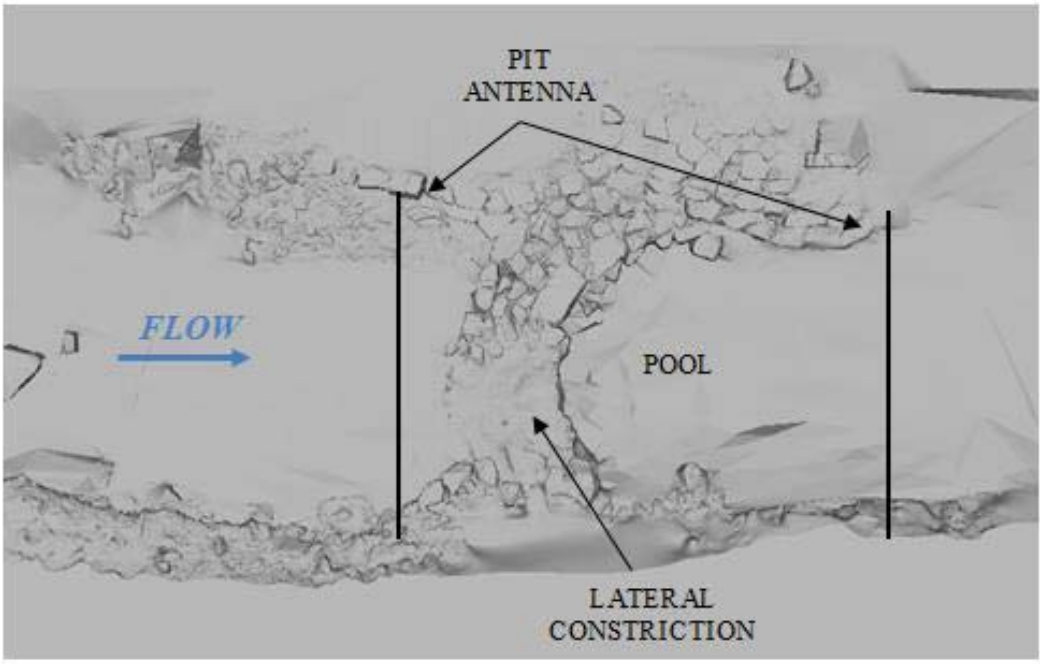

Figure 2.1: Plan view of a WWP structure with PIT-antenna configuration.

Passage success was evaluated over four discrete time windows: October 2011 – March 2012, March 2012 – October 2012, October 2012 – November 2012, and November 2012 – December 2012. The start of each time window was defined by a stocking or electroshocking event in which fish were observed in the pool directly below a structure. Movements were evaluated over the duration of that respective time window. A successful movement across a structure was only included in the analysis if a fish was observed in the pool directly below that structure at the start of the time window. This prevented over estimating passage success at structures where fishes with greater swimming abilities were able to migrate upstream crossing

multiple structures over the duration of a time window. There were 429 successful movements over the duration of all the time windows.

2.2.2 Hydraulic Modeling Results

Seven discharges were modeled at three WWP structures containing fish-tracking data using the 3-D CFD software FLOW-3D® v10.0 (Kolden, 2013). The modeled discharges include: 15, 30, 60, 100, 150, 170, and 300 cfs, representing a range of flows that produce various habitats throughout the year. FLOW-3D described the flow field by solving the Reynolds-Averaged Navier-Stokes (RANS) equations of fluid motion and a default renormalization group (RNG) turbulence closure with dynamically-computed turbulent mixing length. The fluid domain was comprised of a series of discrete points making-up a mesh. The uniform grid sizes of the mesh ranged from 0.125 to 0.5 ft. The free surface was represented in the structured mesh by a process called volume of fluid (VOF) [FLOW Science, 2009], and channel roughness elements were assumed to be adequately resolved through surveyed bathymetry. Model validation through field measurements ensured the model was performing within an acceptable range of error (Kolden, 2013). Additional model validation was infeasible due to severe floods in September 2013 that significantly altered the channel geometry. Post-processing of the hydraulic results from the CFD model was performed using EnSight® Standard v10.0.3.

2.3 Defining the Flow Field

In order to equally compare the hydraulics among WWP structures and across a range of discharges within WWP structures, a physically-based criterion was needed to define the upstream and downstream boundaries of the analysis domain. The Froude number provided a

physically meaningful criterion for establishing boundary conditions that captured the full extent of potential hydraulic barriers to fish passage. The upstream and downstream boundaries were defined by a Froude number of 1 and 0.8, respectively. The upstream boundary condition includes supercritical flow and the most challenging velocities that must be traversed by a fish at all discharges. The downstream boundary encompasses the hydraulic jump from supercritical flow to subcritical flow and the highest levels of turbulence.

EnSight® was used to create a flow volume consisting of the total modeled domain. Additional, reduced flow volumes were created that consisted of the total modeled domain below a specified Froude number (Figure 2.2). The cross-sectional area of the reduced and total flow volumes were sampled at 0.25-ft longitudinal increments throughout the entire reach. A deviation in the cross-sectional area, between the total flow volume and the reduced flow volume, indicated areas with a Froude number greater than the thresholds used to define the boundaries of the analysis domain (Figure 2.3). This process was repeated for all modeled discharges at each structure. The upstream-most point for all discharges at which the cross-sectional areas diverged was used as the upstream boundary, and the downstream-most point at which the cross-sectional areas diverged was used as the downstream boundary. The Froude criteria were thoroughly analyzed to ensure the boundaries captured all features of the flow field relevant to fish passage.

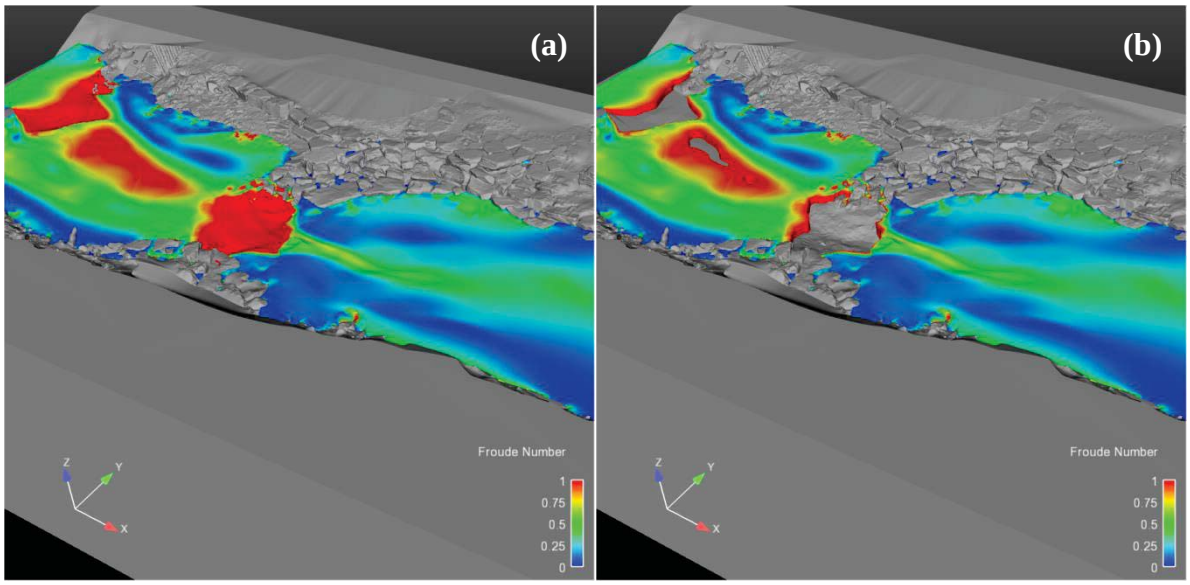

Figure 2.2: (a) Total flow volume, and (b) the reduced flow volume of all Froude numbers less than 1.

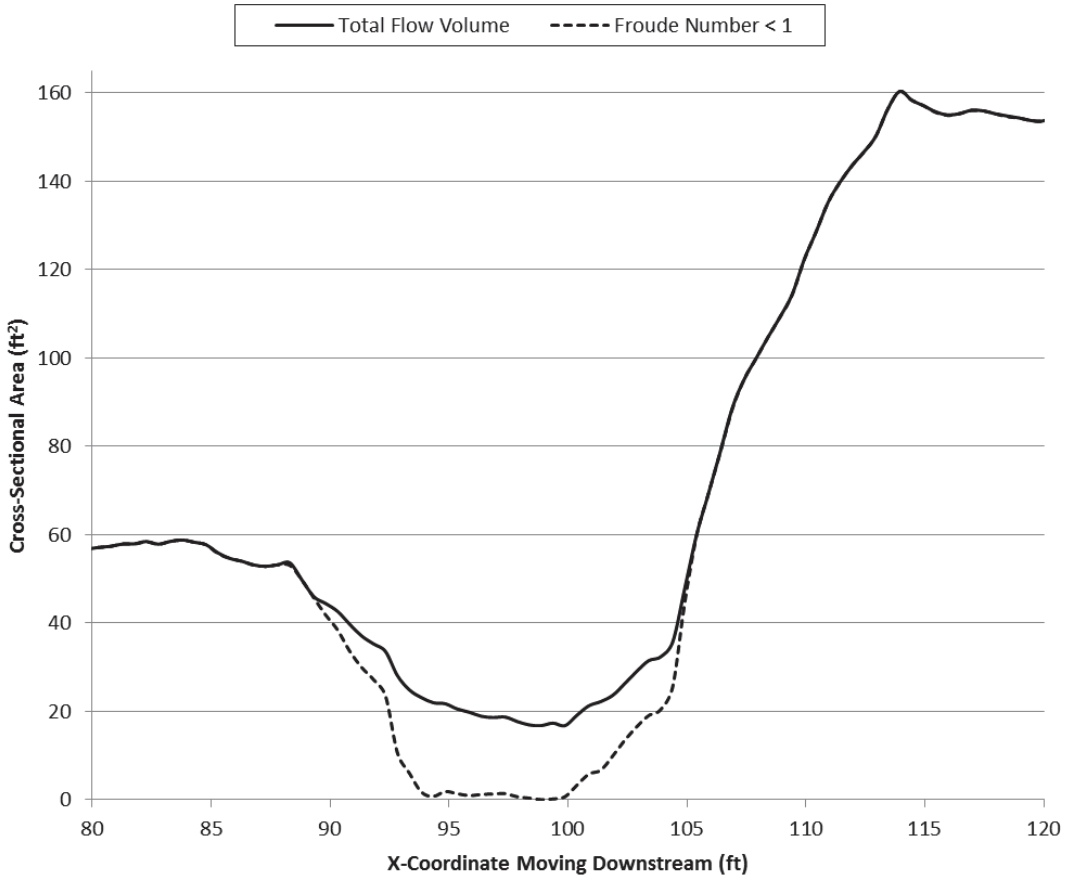

Figure 2.3: Example of longitudinal changes in cross-sectional area of the total flow volume versus the reduced flow volume comprised of Froude numbers less than 1.

2.4 Particle Trace and Potential Swimming Path Development

Releasing particle traces through the flow field and quantifying hydraulic variables along each trace provides a meaningful description of the hydraulic conditions a fish might encounter while migrating upstream. EnSight® was used to emit particle traces from nodes within the gridded mesh. A particle trace consists of a series of points that track a massless-particle through both time and space in the fluid domain. The trajectory of the particle trace is parallel to the velocity vector field at that point and time.

Releasing particle traces from a cross section at the upstream boundary limits the number of particle traces to the number of nodes that make-up the cross section; however, particle traces can be emitted from a volume to greatly increase the number of nodes from which particle traces can be emitted. Additionally, releasing particle traces forward in time through the defined flow volume stops the particle traces at the downstream boundary. This excludes eddies and zones of reverse flow where a particle trace would continue past the downstream boundary and then recirculate back upstream into the defined flow volume (Figure 2.4). Therefore, particle traces were emitted forward and backward in time from volumes at the upstream and downstream boundaries encompassing important hydraulic features and the entirety of the flow field (Figure 2.5).

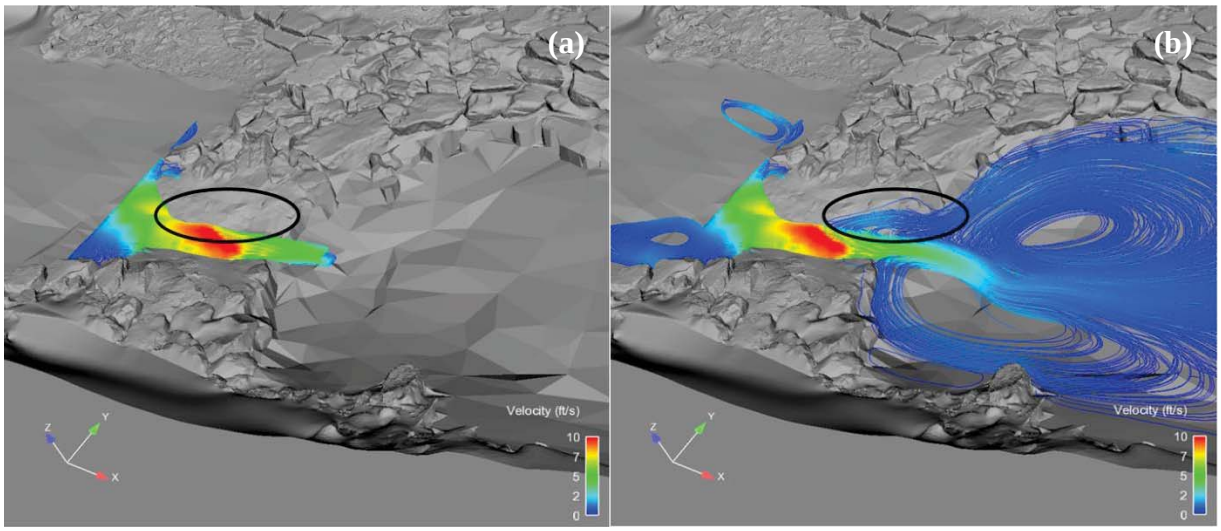

Figure 2.4: (a) Particle traces released forward in time from an upstream cross section traveling to the downstream boundary, and (b) particle traces released forward from an upstream cross section traveling through the entire reach. A reference recirculation zone is highlighted by a circle.

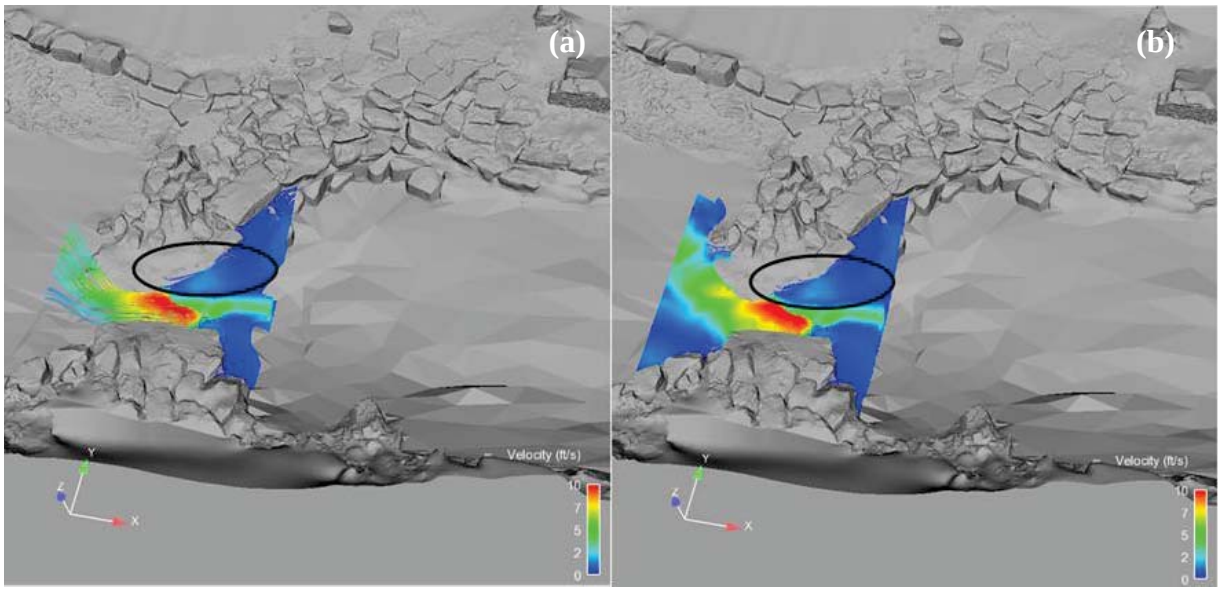

Figure 2.5: (a) Particle traces released from a volume at the downstream boundary both forward and backward in time, and (b) particle traces released from volumes at the upstream and downstream boundaries both forward and backward in time. A reference recirculation zone is highlighted by a circle.

A portion of the particle traces released from volumes at the upstream and downstream boundaries both forward and backward in time nevertheless stopped prematurely and did not reach the opposite boundary. A particle trace stopped prematurely if the trace moved outside the

space in which the vector field was defined or the particle trace entered a location where the velocity was 0 (Computational Engineering International, Inc., 2013). Additional particle traces existed that recirculated in an eddy before stopping prematurely or continuing through the flow field. Particle traces that stopped prematurely or recirculated within the flow volume introduce bias when quantifying hydraulic variables along each particle trace and assessing the conditions a fish might experience as it swims upstream.

In order to resolve this bias, particle traces that recirculated to the upstream or downstream boundary were divided at the point where they began to recirculate relative to the upstream/downstream directions. Two particle traces that do not make it through the entire flow volume result from each circulation. Each trace that did not make it through the entire volume (incomplete trace) was connected to a trace that did travel through the entire flow volume (complete trace) providing a path that represents the hydraulic conditions a fish might experience when migrating upstream. This task was accomplished by searching for the point within all the complete traces with the shortest Euclidean distance to the terminus of an incomplete trace. The new trace consisted of the incomplete trace, the point of connection, and the needed portion of the complete trace to continue through the entire flow volume. The new trace was added to the list of complete traces and made available for connecting to additional incomplete traces. A maximum connection distance of 0.5 ft was established to prevent excessive interpolation and an unrealistic hydraulic representation of the flow field. If the closest connection point for an incomplete trace was greater than 0.5 ft, connecting that particular incomplete trace was re-attempted after all the incomplete traces were cycled through. After the first iteration, the allowable connection distance was adjusted to 1 ft and the process was repeated until the minimum connection distance was greater than 1 ft or there were no more incomplete traces. The

distance of each particle trace was determined along with the maximum distance between nodes along each trace to validate the modified particle traces. Approximately 6,500 to 20,000 particle traces were used to describe the flow field at each structure depending on the flow volume being analyzed.

2.5 Particle Trace Evaluation

Each particle trace was evaluated as a potential fish movement path (flow path). Velocity, depth, vorticity, and TKE were defined in 3-D at every point along a flow path and used to define hydraulic variables that relate to fish swimming abilities. The maximum velocity relative to fish swimming ability, a cumulative cost in terms of energy and the drag force on a fish, the minimum depth, and the sum and maximum vorticity and TKE were quantified along the entire length of each flow path providing a distribution of hydraulic variables for each modeled discharge. The magnitude and distribution of these hydraulic variables were compared among WWP structures.

2.5.1 Velocity

The magnitude of a velocity vector was calculated as the root-mean-square (*rms*) of velocity in the *x*, *y*, and *z* planes with a directional component relative to the *x*-direction (Equation (2.1)):

$$v_{rms} = \sqrt{v_x^2 + v_y^2 + v_z^2} \times \left(\frac{|v_x|}{v_x} \right) \qquad \textbf{Equation (2.1)}$$

By definition, the *rms* of velocity is always positive and does not take into account the direction of flow. This is important because a velocity vector with a resultant in the positive upstream direction might be advantageous to a fish migrating upstream. Therefore, positive and

negative signs were assigned to the v_{rms} based on the velocity in the downstream (v_x) and upstream directions, respectively (Figure 2.6). A positive value indicates a resultant in the downstream direction, while a negative value indicates a resultant in the upstream direction. Velocity vectors that were limited to the *y* (v_y) and *z* (v_z) planes were assigned a positive value.

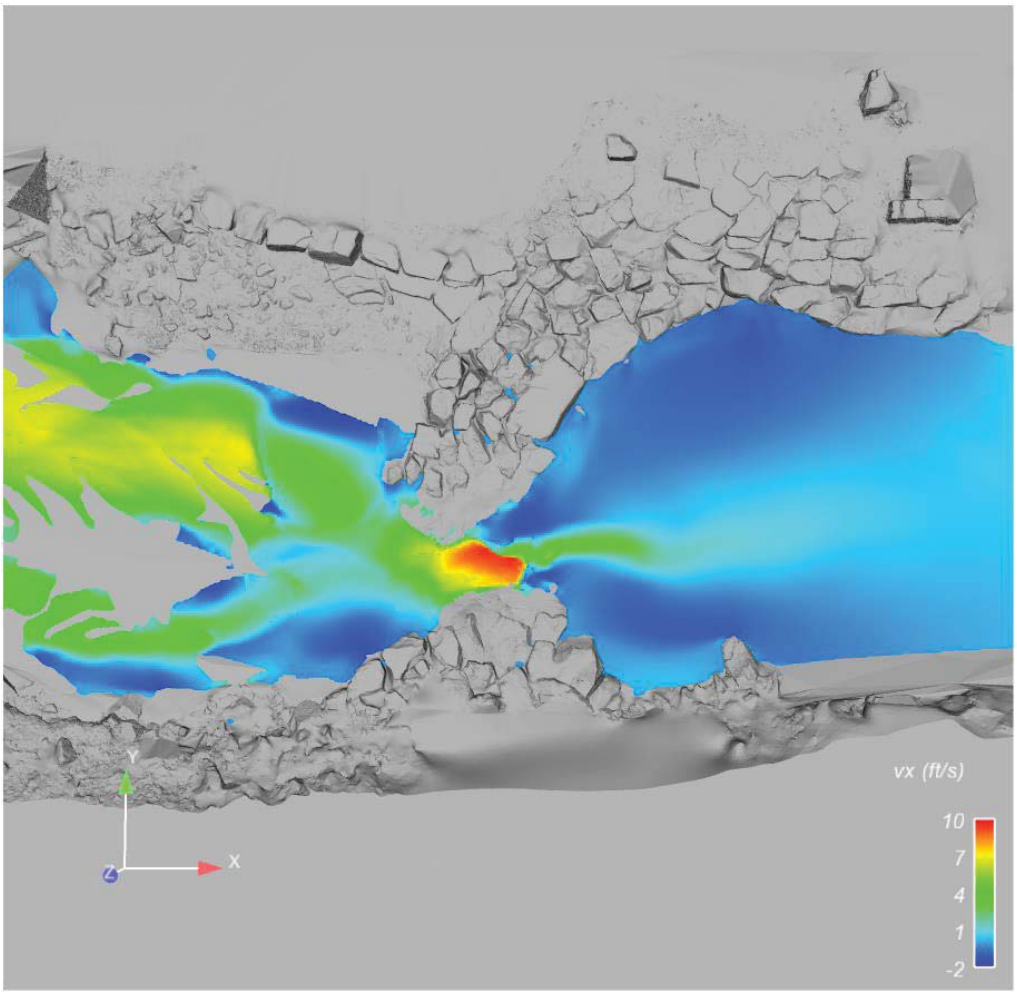

Figure 2.6: Plan view of a WWP structure colored by velocity along the *x*-axis indicating flow moving upstream or downstream.

Velocity was used to define a variable that assesses the hydraulic environment relative to burst swimming ability. The velocity ratio is defined as the ratio of the local water velocity (v_{rms}) to the burst swimming ability (v_{burst}) of a particular fish (Equation (2.2)):

$$\text{velocity ratio} = \frac{v_{rms}}{v_{burst}} \qquad \textbf{Equation (2.2)}$$

This variable is evaluated at every point along a flow path. If the ratio is ≥ 1, theoretically the fish cannot traverse that point. The maximum velocity ratio was determined along each flow path and the fraction of traces with a maximum velocity ratio ≥ 1 was determined. If this fraction equals 1, every trace contains a point greater than a fish's burst swimming ability. If this fraction is 0, theoretically, none of the flow paths are greater than a fish's burst swimming ability. The maximum velocity ratio was determined for 100 – 400 mm fish with burst swimming abilities of 10 and 25 BL/s (Peake *et al*., 1997; Castro-Santos *et al*., 2013).

Velocity was also used to define a cost variable (Equation (2.3)) in order to compare relative measures of cumulative energy expenditure through the length of a structure:

$$\text{Cost} = \int v_{rms}^2 \cdot d \cdot \left(\frac{v_{rms}}{|v_{rms}|} \right) \qquad \textbf{Equation (2.3)}$$

where v_{rms} is the average *rms* velocity between two nodes; and d is the distance between two nodes. The square of velocity is proportional to energy and the drag force on a fish (Chow, 1959; McElroy *et al*., 2012). The distance term accounts for the length over which a fish might experience those velocities. By squaring the v_{rms}, it is always positive; thus, the fraction term containing the v_{rms} adds a directional component to the cost based on the upstream/downstream directions. If the flow is traveling downstream, the cost between nodes will be positive as a fish will have to expend more energy to swim against the flow and vice versa. Cost is calculated over the distance in between nodes and summed along the length of the flow path. Therefore, the length of the hydraulic jump at a structure has a direct effect on cost.

2.5.2 Depth

A minimum of 0.6 ft was used to evaluate depth as a barrier to upstream passage for this study. Without direct knowledge of fish body depths, 0.6 ft provides an average minimum depth criterion across the range of suggested values and fish size (Hotchkiss and Frei, 2007). Any location along a flow path where the fluid was less than 0.6 ft was defined as a passage barrier. The minimum fluid depth along each flow path was evaluated, and the fraction of flow paths that did not maintain at least 0.6 ft along the entire length of the path was determined. The maximum velocity ratio and depth were also assessed in combination. If the minimum depth along a flow path was less than 0.6 ft or the maximum velocity along the path was greater than a fish's swimming ability, the flow path was considered a passage barrier. Each flow path was evaluated, and the fraction of flow paths that exceeded a fish's burst swimming ability or did not provide adequate depth was determined.

2.5.3 Turbulence

Vorticity and TKE were selected as measures of turbulence meaningful to a fish. Vorticity is a vector representing the rotation rate of a small fluid element about its axis (Crowder and Diplas, 2002; Kolden, 2013). EnSight® was used to calculate 3-D vorticity at each element within the gridded mesh (Equation (2.4)):

$$\vec{\xi} = \left(\frac{\partial w}{\partial y} - \frac{\partial v}{\partial z}\right)\hat{i} + \left(\frac{\partial u}{\partial z} - \frac{\partial w}{\partial x}\right)\hat{j} + \left(\frac{\partial v}{\partial x} - \frac{\partial u}{\partial y}\right)\hat{k} \qquad \textbf{Equation (2.4)}$$

where u, v, and w are the x, y, and z-components of velocity, respectively, and i, j, and k are unit vectors in the x, y, and z directions, respectively. TKE is a measure of the increase in kinetic energy due to turbulent velocity fluctuations in the flow (Equation (2.5)) (Lacey *et al*., 2012; FLOW Science, 2009):

$$\mathrm{TKE} = \frac{1}{2}\left(\sigma_u^2 + \sigma_v^2 + \sigma_w^2\right) \qquad \textbf{Equation (2.5)}$$

where σ_u, σ_v, and σ_w are the standard deviations of velocity in the x, y, and z directions, respectively.

The magnitudes of vorticity and TKE at each point along a flow path were summed over the length of the path quantifying the cumulative effect of vorticity and TKE a fish might experience. Additionally, the maximum vorticity and TKE along the length of a path was determined to examine the largest magnitudes of vorticity and TKE a fish might experience. Specific thresholds of turbulence relative to fish swimming abilities are unknown; therefore, we are limited to a relative comparison of turbulence among WWP structures and passage success. Examining the cumulative effect and maximum magnitudes of vorticity and TKE along each flow path highlights potential barriers due to turbulence cumulatively through the flow volume and in locations characterized by the highest levels of turbulence.

2.6 Data Analysis

Individual fish were designated as making a successful movement or an unsuccessful movement for each time window. The hydraulic variables associated with a successful movement were determined based on the discharge at which the movement occurred. However, the hydraulic variables associated with an unsuccessful movement were determined based on the most frequent discharge that occurred during the respective time window. Logistic regression was used to test for a significant influence of the hydraulic variables on passage success. Significance was evaluated using the chi-square statistic. Stepwise forward regression with a minimum Akaike Information Criterion (AIC) stopping rule was used to determine the hydraulic variables to include in logistic regression. Collinearity was assessed by examining the bivariate

fits among the hydraulic variables. To avoid issues of collinearity, combinations of variables were manually selected to be tested for significance by stepwise forward regression. All statistical procedures were completed using JMP® Pro 11 (SAS Institute Inc., 2013).

CHAPTER 3 RESULTS

Quantifying the hydraulic conditions along potential fish swimming paths highlights the magnitude and distribution of potential barriers to upstream migrating trout at each WWP structure. The magnitude and distribution of the hydraulic variables vary among WWP structures, relative to each size class of fish, and across discharges, similar to passage success. Further, logistic regression shows a statistically significant influence of specific hydraulic variables on passage success.

3.1 Hydraulic Variables

WWP1 is the most downstream structure characterized by a short-steep drop constructed by large boulders. WWP2 is the middle structure producing a wave over a longer distance with the maximum constriction at the exit of the chute into the downstream pool. WWP3 is the most upstream structure producing a wave similar to WWP2 but over a longer chute. The total length of the flow volume from the upstream to downstream boundary was 11 ft at WWP1, 16.5 ft at WWP2, and 19.6 ft at WWP3 (Figure 3.1).

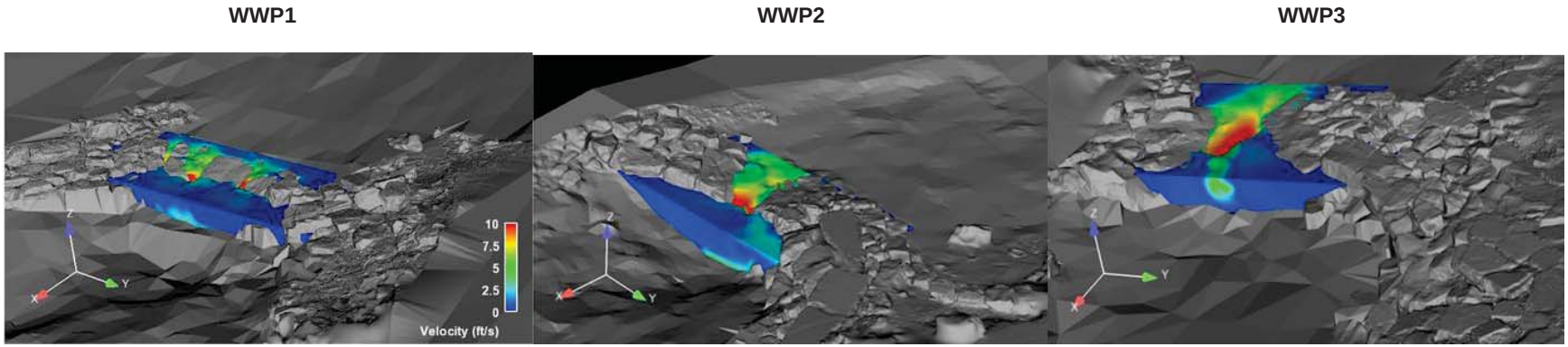

(a) 15 cfs

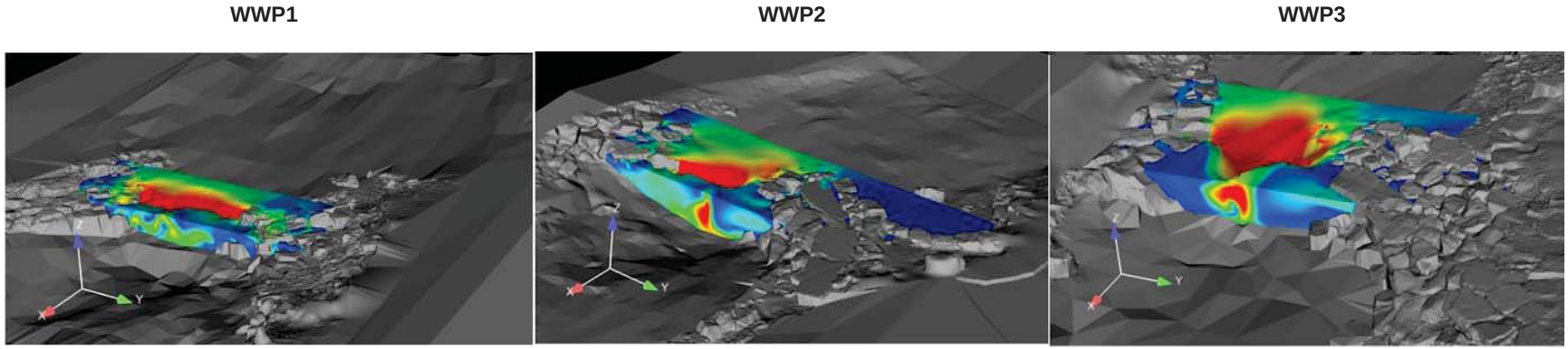

(b) 150 cfs

Figure 3.1: Analysis flow volume at WWP1, WWP2, and WWP3 for (a) 15 cfs, and (b) 150 cfs.

3.1.1 Maximum Velocity Ratio

The fraction of flow paths that exceed a fish's burst swimming ability varies among WWP structures, different size classes of fish, and across discharges (Tables 3.1 and 3.2). For example, assuming a burst velocity of 25 BL/s at WWP1 indicates that there are more flow paths available (flow paths that are not barriers to migration) at 15 cfs compared to 300 cfs for a 125-mm fish. In contrast, there are more flow paths available at 300 cfs compared to 15 cfs for a 150-mm fish. This relationship varies among structures, where there are more flow paths available at 15 cfs compared to 300 cfs for a 150-mm fish at WWP2 and WWP3 (Table 3.1). This variability is also present for burst swimming abilities of 10 BL/s (Table 3.2).

The results for 25 BL/s indicate that a majority of the flow paths are available at all discharges for 175-mm fish and larger (Table 3.1). Though few flow paths are available, WWP1 provides the most available flow paths for the smallest size class of fish compared to WWP2 and WWP3, with a majority of the traces becoming available for fish 150 mm and larger. At WWP2, greater than 20 percent of the flow paths at 30 cfs exceed the swimming ability of fish up to 300 mm in length. A large number of flow paths become available for fish exceeding 175 mm in length across all discharges at WWP2, with the exception of 30 cfs. In general, there are more available flow paths across discharges and size classes of fish at WWP3, with a majority of the flow paths becoming available for fish exceeding 150 mm in length. WWP2 appears to present the fewest available flow paths. There is a general trend at all WWP structures for fish less than 175 mm in length that neither the lowest nor highest discharge presents the greatest challenge; rather, an intermediate discharge appears to be most limiting.

Table 3.1: Fraction of traces that exceed burst swimming abilities (25 BL/s) for each size class, discharge, and WWP structure.

		Fish Body Length												
	Discharge (cfs)	100 mm	125 mm	150 mm	175 mm	200 mm	225 mm	250 mm	275 mm	300 mm	325 mm	350 mm	375 mm	400 mm
WWP1	15	0.89	0.2	0.12	0.07	0.02	0.02	0	0	0	0	0	0	0
	30	1	0.44	0.12	0.08	0.01	0	0	0	0	0	0	0	0
	60	1	0.28	0.13	0.06	0.05	0	0	0	0	0	0	0	0
	100	1	0.95	0.21	0.07	0	0	0	0	0	0	0	0	0
	150	0.99	0.9	0.1	0.03	0.03	0	0	0	0	0	0	0	0
	170	0.98	0.86	0.35	0.09	0	0	0	0	0	0	0	0	0
	300	0.96	0.54	0.05	0.01	0	0	0	0	0	0	0	0	0
WWP2	15	1	0.85	0.11	0	0	0	0	0	0	0	0	0	0
	30	1	1	0.39	0.25	0.23	0.23	0.23	0.23	0.23	0.03	0.03	0.03	0
	60	1	1	1	0.19	0.01	0	0	0	0	0	0	0	0
	100	1	0.97	0.62	0.28	0.17	0	0	0	0	0	0	0	0
	150	1	0.76	0.62	0.15	0	0	0	0	0	0	0	0	0
	170	1	0.99	0.45	0.2	0.07	0	0	0	0	0	0	0	0
	300	1	0.98	0.23	0.03	0	0	0	0	0	0	0	0	0
WWP3	15	1	0.07	0	0	0	0	0	0	0	0	0	0	0
	30	1	0.07	0	0	0	0	0	0	0	0	0	0	0
	60	1	0.27	0	0	0	0	0	0	0	0	0	0	0
	100	1	0.83	0.36	0.01	0	0	0	0	0	0	0	0	0
	150	1	0.9	0.5	0	0	0	0	0	0	0	0	0	0
	170	0.57	0.55	0.27	0.07	0	0	0	0	0	0	0	0	0
	300	1	0.76	0.34	0.01	0	0	0	0	0	0	0	0	0

Table 3.2: Fraction of traces that exceed burst swimming abilities (10 BL/s) for each size class, discharge, and WWP structure.

		Fish Body Length												
	Discharge (cfs)	100 mm	125 mm	150 mm	175 mm	200 mm	225 mm	250 mm	275 mm	300 mm	325 mm	350 mm	375 mm	400 mm
WWP1	15	1	1	1	1	1	0.93	0.89	0.75	0.53	0.16	0.12	0.12	0.11
	30	1	1	1	1	1	1	1	0.75	0.58	0.39	0.2	0.12	0.09
	60	1	1	1	1	1	1	1	0.99	0.96	0.26	0.17	0.13	0.12
	100	1	1	1	1	1	1	1	1	0.96	0.93	0.62	0.21	0.12
	150	1	1	1	1	1	1	0.99	0.94	0.92	0.86	0.48	0.1	0.07
	170	1	1	1	1	1	1	0.98	0.92	0.88	0.81	0.7	0.35	0.23
	300	1	1	1	1	1	0.99	0.96	0.84	0.62	0.44	0.18	0.05	0.01
WWP2	15	1	1	1	1	1	1	1	1	0.88	0.25	0.15	0.11	0.06
	30	1	1	1	1	1	1	1	1	1	1	0.45	0.39	0.28
	60	1	1	1	1	1	1	1	1	1	1	1	1	0.88
	100	1	1	1	1	1	1	1	0.99	0.98	0.71	0.69	0.62	0.47
	150	1	1	1	1	1	1	1	1	0.76	0.72	0.67	0.62	0.36
	170	1	1	1	1	1	1	1	1	1	0.6	0.58	0.45	0.32
	300	1	1	1	1	1	1	1	1	0.99	0.95	0.35	0.23	0.08
WWP3	15	1	1	1	1	1	1	1	0.51	0.14	0.01	0	0	0
	30	1	1	1	1	1	1	1	0.96	0.61	0	0	0	0
	60	1	1	1	1	1	1	1	0.68	0.65	0.04	0.01	0	0
	100	1	1	1	1	1	1	1	0.87	0.84	0.76	0.57	0.36	0.26
	150	1	1	1	1	1	1	1	0.98	0.96	0.74	0.64	0.5	0.1
	170	1	1	1	1	1	0.82	0.57	0.57	0.56	0.5	0.35	0.27	0.17
	300	1	1	1	1	1	1	1	1	0.81	0.74	0.67	0.34	0.24

When examining burst swimming abilities of 10 BL/s, greater than 90 percent of the flow paths exceed a fish's burst swimming ability at all structures for fish 200 mm and smaller (Table 3.2). WWP1 and WWP2 vary in the fraction of available flow paths depending on the discharge and size class of fish; however, there is a general tendency that fewer flow paths are available at WWP2 compared to WWP1. At WWP2, there are no available flow paths for fish ≤ 325 mm at 30 cfs and ≤ 375 mm at 60 cfs. Larger fish consistently have the most available flow paths at WWP3. A threshold appears at WWP3 with a large fraction of flow paths

becoming available at 15 to 60 cfs. Again, there is a general tendency that neither the lowest nor the highest discharge presents the greatest challenge.

3.1.2 Depth

The fraction of flow paths that do not provide adequate depth for fish passage varies among WWP structure and discharge; however, low flows appear to be the most limiting (Figure 3.2). At 15 cfs, WWP2 and WWP3 do not have any flow depths greater than 0.6 ft, while greater than 90 percent of the flow paths contain depths less than 0.6 ft at WWP1. WWP1 poses the greatest depth challenge at intermediate flows with greater than 60 percent of the flow paths inaccessible due to depth. At high flows, the fraction of available flow paths increase at WWP1 and WWP3 reducing the likelihood of depth as a passage barrier. At WWP2, the fraction of flow paths acting as a depth barrier increases from 40 percent at 150 cfs to 65 percent at 300 cfs.

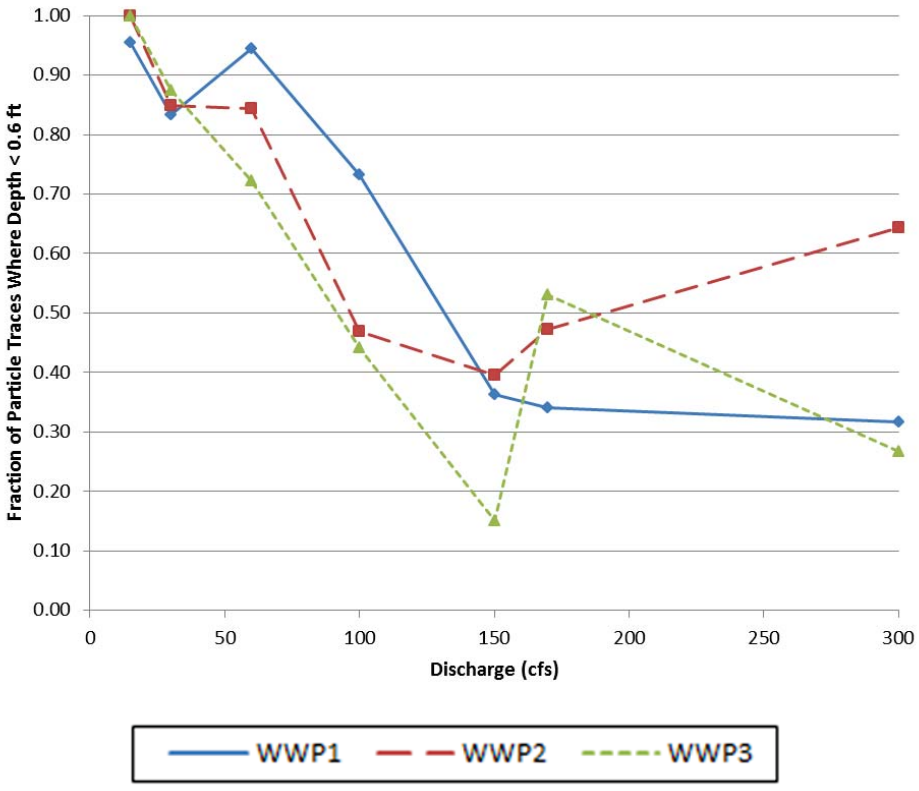

Figure 3.2: The fraction of flow paths where the minimum depth is less than 0.6 ft for each discharge and WWP structure.

3.1.3 Maximum Velocity Ratio and Depth Combined

The fraction of flow paths that either exceed a fish's burst swimming ability or do not provide adequate flow depth varies among WWP structure, size class of fish, and across discharges. Simultaneously examining the maximum velocity ratio for 25 BL/s and depth shows that greater than 80 percent of the flow paths are inaccessible to fish of all size classes at flows less than 30 cfs (Table 3.3). In general, WWP1 provides the most available flow paths for fish 150 mm in length and less. WWP1 has the largest fraction of available flow paths at 15 and 30 cfs while WWP3 has the least available flow paths. Flows greater than 150 cfs provide the most available flow paths at all structures.

Table 3.3: Fraction of traces that exceed burst swimming abilities based on the minimum depth criterion and maximum velocity ratio (25 BL/s) for each size class, discharge, and WWP structure.

		Fish Body Length												
	Discharge (cfs)	100 mm	125 mm	150 mm	175 mm	200 mm	225 mm	250 mm	275 mm	300 mm	325 mm	350 mm	375 mm	400 mm
WWP1	15	1	0.95	0.95	0.95	0.95	0.95	0.95	0.95	0.95	0.95	0.95	0.95	0.95
	30	1	0.98	0.88	0.87	0.83	0.83	0.83	0.83	0.83	0.83	0.83	0.83	0.83
	60	1	1	0.95	0.95	0.95	0.95	0.95	0.95	0.94	0.94	0.94	0.94	0.94
	100	1	0.99	0.78	0.73	0.73	0.73	0.73	0.73	0.73	0.73	0.73	0.73	0.73
	150	1	0.99	0.39	0.36	0.36	0.36	0.36	0.36	0.36	0.36	0.36	0.36	0.36
	170	1	0.96	0.55	0.34	0.34	0.34	0.34	0.34	0.34	0.34	0.34	0.34	0.34
	300	1	0.73	0.36	0.32	0.32	0.32	0.32	0.32	0.32	0.32	0.32	0.32	0.32
WWP2	15	1	1	1	1	1	1	1	1	1	1	1	1	1
	30	1	1	0.91	0.86	0.85	0.85	0.85	0.85	0.85	0.85	0.85	0.85	0.85
	60	1	1	1	0.89	0.85	0.84	0.84	0.84	0.84	0.84	0.84	0.84	0.84
	100	1	1	1	0.72	0.64	0.47	0.47	0.47	0.47	0.47	0.47	0.47	0.47
	150	1	1	0.96	0.54	0.4	0.4	0.4	0.4	0.4	0.4	0.4	0.4	0.4
	170	1	1	0.9	0.66	0.55	0.47	0.47	0.47	0.47	0.47	0.47	0.47	0.47
	300	1	1	0.81	0.67	0.64	0.64	0.64	0.64	0.64	0.64	0.64	0.64	0.64
WWP3	15	1	1	1	1	1	1	1	1	1	1	1	1	1
	30	1	0.88	0.87	0.87	0.87	0.87	0.87	0.87	0.87	0.87	0.87	0.87	0.87
	60	1	0.92	0.72	0.72	0.72	0.72	0.72	0.72	0.72	0.72	0.72	0.72	0.72
	100	1	1	0.78	0.45	0.44	0.44	0.44	0.44	0.44	0.44	0.44	0.44	0.44
	150	1	1	0.65	0.16	0.15	0.15	0.15	0.15	0.15	0.15	0.15	0.15	0.15
	170	1	1	0.79	0.6	0.53	0.53	0.53	0.53	0.53	0.53	0.53	0.53	0.53
	300	1	1	0.61	0.28	0.27	0.27	0.27	0.27	0.27	0.27	0.27	0.27	0.27

Combining the minimum flow depth and the maximum velocity ratio for 10 BL/s as barriers to migration indicates that greater than 90 percent of the flow paths are unavailable for fish less than 300 mm in length (Table 3.4). In general, WWP2 provides the fewest number of available flow paths. Excluding 15 cfs, there is an evident threshold at WWP3 that all flow paths are inaccessible for fish 300 mm in length and smaller. At WWP1 and WWP2, a clear threshold for the size class of fish at which flow paths become accessible is less apparent as discharge varies.

Table 3.4: Fraction of traces that exceed burst swimming abilities based on the minimum depth criterion and maximum velocity ratio (10 BL/s) for each size class, discharge, and WWP structure.

		Fish Body Length												
	Discharge (cfs)	100 mm	125 mm	150 mm	175 mm	200 mm	225 mm	250 mm	275 mm	300 mm	325 mm	350 mm	375 mm	400 mm
WWP1	15	1	1	1	1	1	1	1	1	0.96	0.95	0.95	0.95	0.95
	30	1	1	1	1	1	1	1	1	1	0.97	0.88	0.88	0.87
	60	1	1	1	1	1	1	1	1	1	0.99	0.95	0.95	0.95
	100	1	1	1	1	1	1	1	1	0.99	0.98	0.87	0.78	0.74
	150	1	1	1	1	1	1	1	0.99	0.99	0.96	0.67	0.39	0.37
	170	1	1	1	1	1	1	1	1	0.98	0.93	0.86	0.55	0.45
	300	1	1	1	1	1	1	1	0.97	0.8	0.65	0.43	0.36	0.33
WWP2	15	1	1	1	1	1	1	1	1	1	1	1	1	1
	30	1	1	1	1	1	1	1	1	1	1	0.96	0.91	0.89
	60	1	1	1	1	1	1	1	1	1	1	1	1	0.96
	100	1	1	1	1	1	1	1	1	1	1	1	1	0.89
	150	1	1	1	1	1	1	1	1	1	1	1	0.96	0.7
	170	1	1	1	1	1	1	1	1	1	1	0.98	0.9	0.77
	300	1	1	1	1	1	1	1	1	1	0.99	0.92	0.81	0.7
WWP3	15	1	1	1	1	1	1	1	1	1	1	1	1	1
	30	1	1	1	1	1	1	1	1	0.96	0.88	0.87	0.87	0.87
	60	1	1	1	1	1	1	1	1	1	0.75	0.72	0.72	0.72
	100	1	1	1	1	1	1	1	1	1	0.99	0.97	0.78	0.68
	150	1	1	1	1	1	1	1	1	1	0.86	0.76	0.65	0.25
	170	1	1	1	1	1	1	1	1	1	0.97	0.87	0.79	0.7
	300	1	1	1	1	1	1	1	1	1	1	0.94	0.61	0.5

3.1.4 Cost

The magnitude and distribution of cost vary among WWP structures and discharges (Figure 3.3). WWP1 consistently has a lower cost at all discharges. WWP2 and WWP3 have similar magnitudes of cost at 15 and 30 cfs. The distribution of cost is much narrower at 15 cfs. WWP3 has the maximum 50th percentile of cost at all discharges except 60 cfs (Figure 3.4). At 100 cfs, the range of costs at WWP3 increases and indicates greater hydraulic heterogeneity

within the flow field. The maximum cost at WWP2 occurs at 30 cfs. At 150 and 300 cfs, the maximum cost at WWP1 greatly increases.

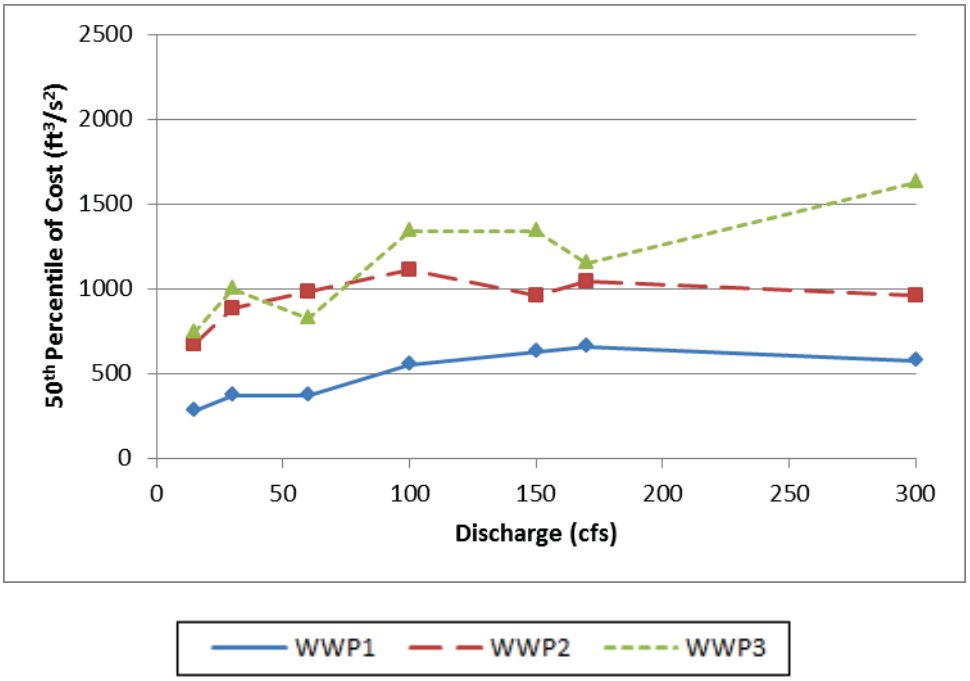

Figure 3.3: 50th percentile of cost for each WWP structure and discharge.

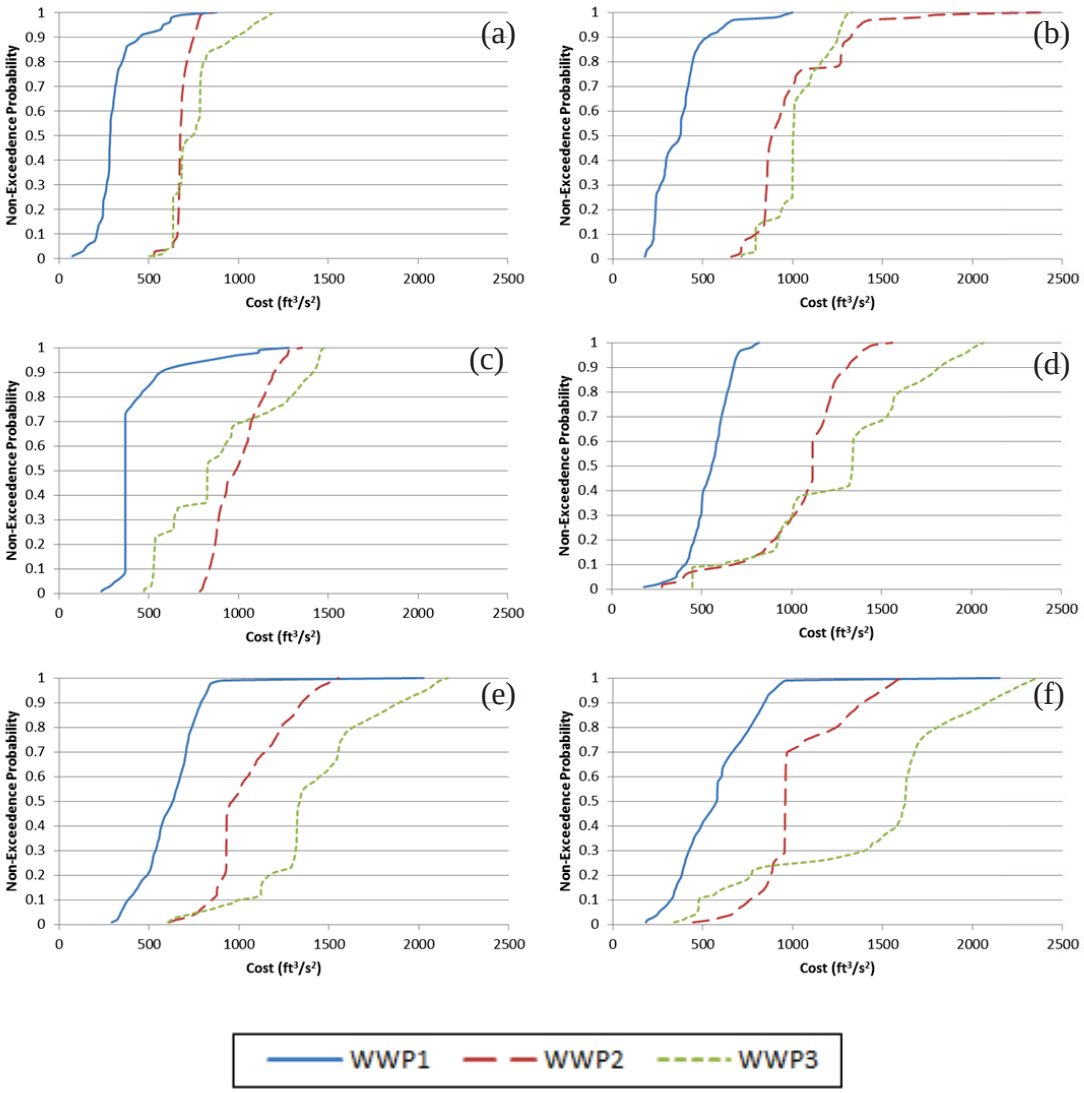

Figure 3.4: Non-exceedence probabilities for the cost along flow paths at each WWP structure for: (a) 15 cfs, (b) 30 cfs, (c) 60 cfs, (d) 100 cfs, (e) 150 cfs, and (f) 300 cfs.

3.1.5 Turbulence

The highest magnitudes and broader distributions of the maximum vorticity generally occur at the lowest discharges (15 and 30 cfs). WWP3 has the greatest 50th percentile of maximum vorticity at 15 and 30 cfs (Figure 3.5); however, WWP1 has the highest overall maximum vorticity value at 30 cfs (Figure 3.5). The magnitude and distribution of the maximum vorticity is similar among the WWP structures at discharges ≥ 100 cfs.

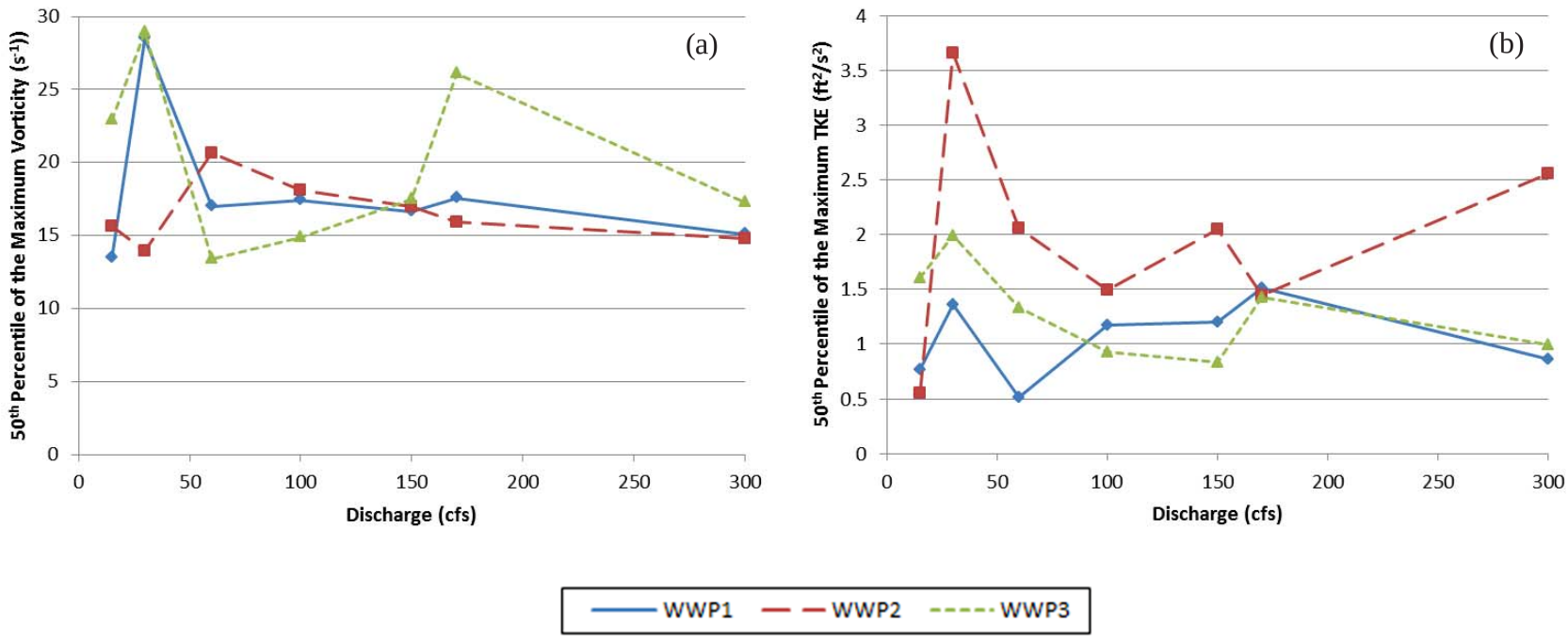

Figure 3.5: 50th percentile of the (a) maximum vorticity, and (b) maximum TKE along a flow path for each WWP structure and discharge.

The magnitude and distribution of the maximum TKE along a flow path also vary substantially among WWP structures and discharges (Figure 3.6). At a specific discharge, the maximum TKE among the WWP structures depends on the percentile of the distribution. WWP1 has the highest maximum TKE at 30, 100, and 300 cfs. WWP2 has the greatest 50th percentile of TKE at all discharges except 30 cfs (Figure 3.7). WWP3 appears to have a more narrow distribution of TKE at all discharges compared to WWP1 and WWP2. The maximum 50th percentile of TKE occurs at 30 cfs at WWP2 and WWP3, and 170 cfs at WWP1.

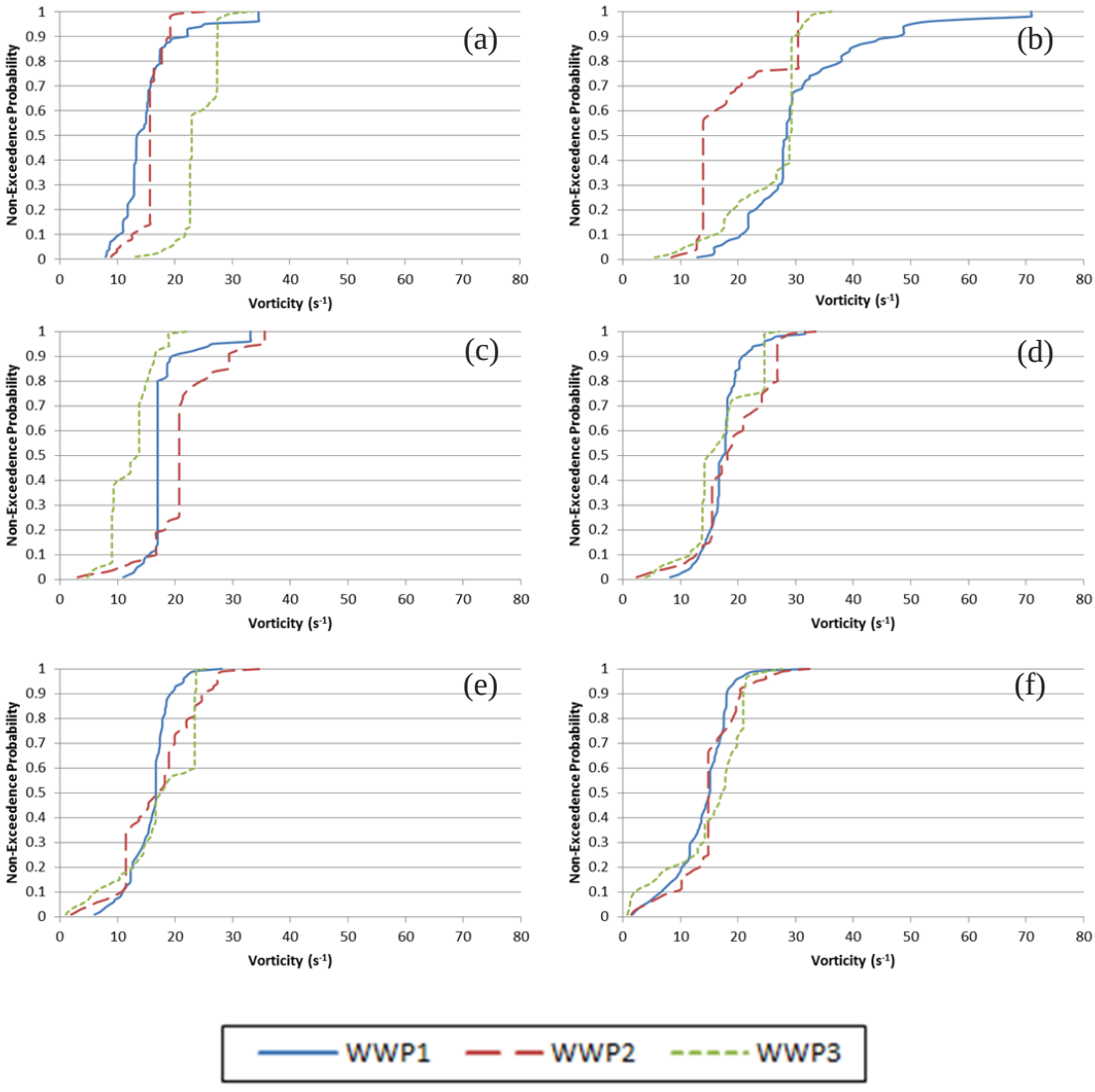

Figure 3.6: Non-exceedence probabilities for maximum vorticity along flow paths at each WWP structure for: (a) 15 cfs, (b) 30 cfs, (c) 60 cfs, (d) 100 cfs, (e) 150 cfs, and (f) 300 cfs.

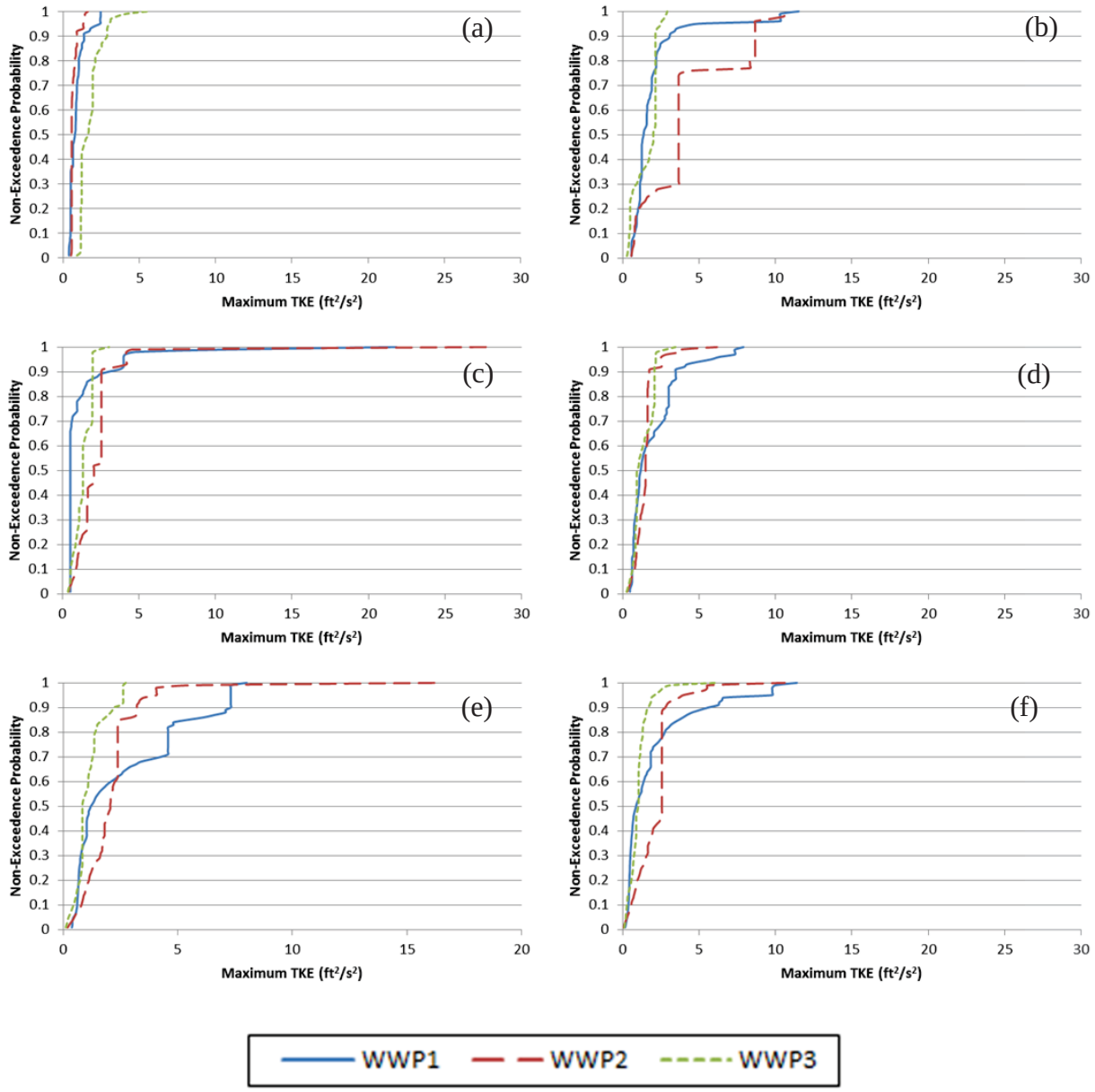

Figure 3.7: Non-exceedence probabilities for the maximum TKE along flow paths at each WWP structure for: (a) 15 cfs, (b) 30 cfs, (c) 60 cfs, (d) 100 cfs, (e) 150 cfs, and (f) 300 cfs.

The magnitude and distribution of the sum of vorticity along a flow path vary among WWP structures and discharges (Figure 3.8). The maximum 50th percentile of the sum of vorticity along a flow path occurs at 30 cfs for WWP1 and WWP3, and 100 cfs for WWP2 (Figure 3.8). WWP3 has the highest 50th percentile of the sum of vorticity with the exception of 60 and 100 cfs. The maximum of the sum of vorticity along a flow path varies between WWP2

and WWP3 depending on the discharge and percentile being analyzed. There is a general trend that WWP1 contains the lowest sum of vorticity along a flow path. Additionally, narrow distributions for each WWP exist at 15, 150, and 300 cfs.

The magnitude and distribution of the sum of TKE along a flow path varies among WWP structures and discharges (Figure 3.9). The maximum 50^{th} percentile of the sum of TKE occurs at 30 cfs for WWP1 and WWP3, and 300 cfs for WWP2 (Figure 3.10). Similar trends in the relative magnitude of the 50^{th} percentile of the sum of vorticity and TKE exist at each individual WWP structure. The 50^{th} percentile of the sum of TKE is lowest at WWP1 for all discharges. However, WWP1 has the overall maximum of the sum of TKE along a flow path at 150 and 300 cfs, while WWP2 had the overall maximum at 30 to 100 cfs. WWP3 has the overall maximum of the sum of TKE along a flow path at 15 cfs. Each structure is characterized by a narrower distribution of the sum of TKE at 15 cfs.

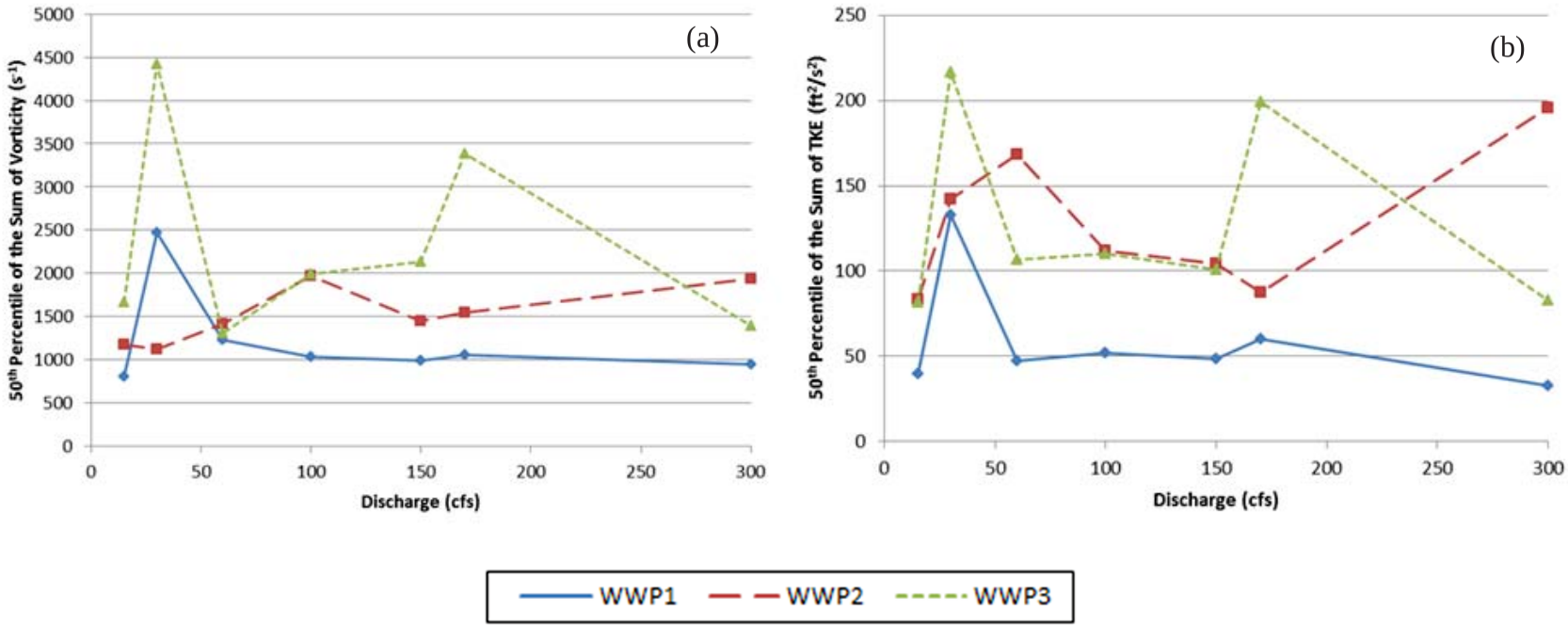

Figure 3.8: 50th percentile of the (a) sum of vorticity, and (b) TKE along a flow path for each WWP structure and discharge.

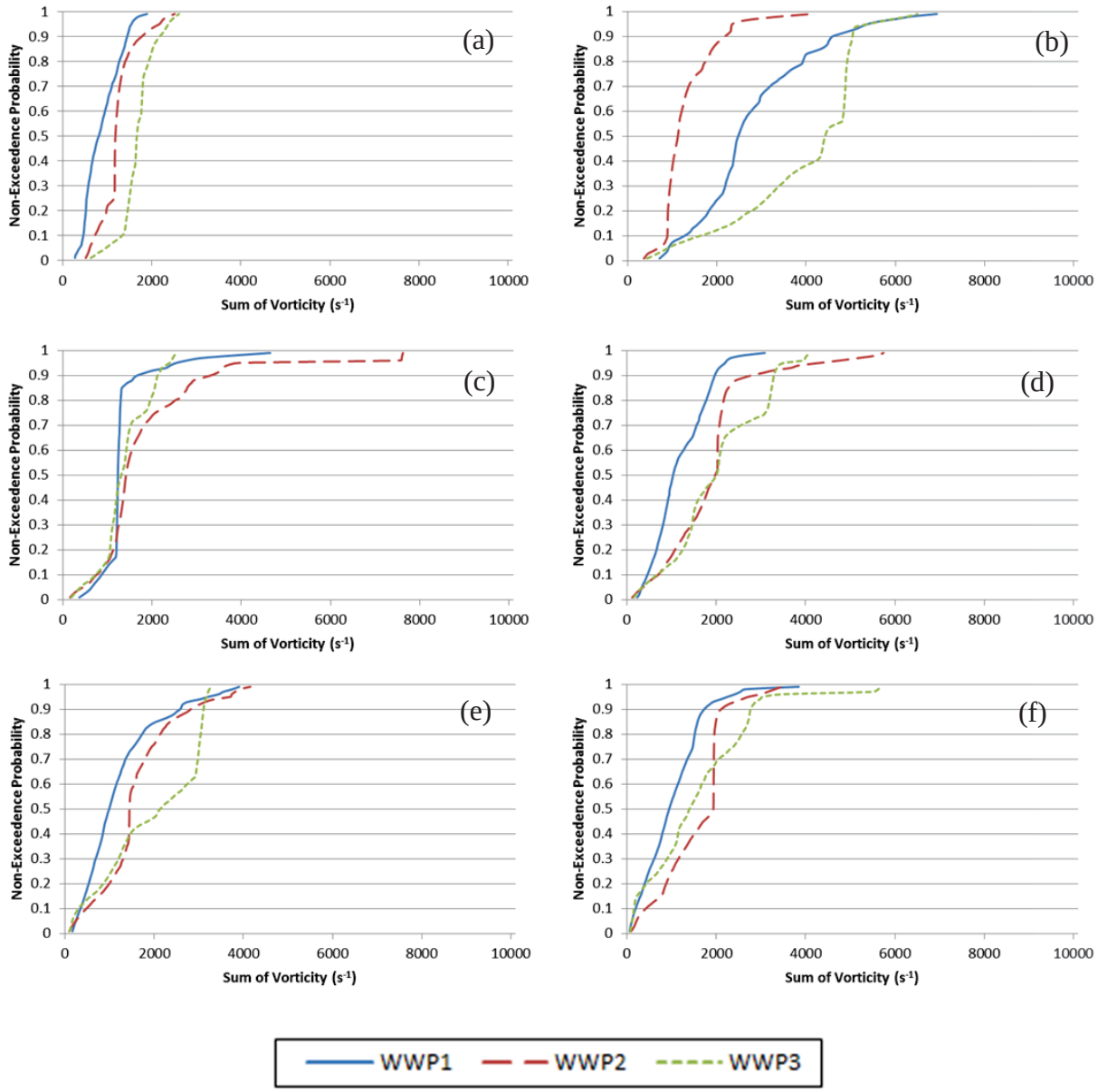

Figure 3.9: Non-exceedence probabilities for sum of vorticity along flow paths at each WWP structure for: (a) 15 cfs, (b) 30 cfs, (c) 60 cfs, (d) 100 cfs, (e) 150 cfs, and (f) 300 cfs.

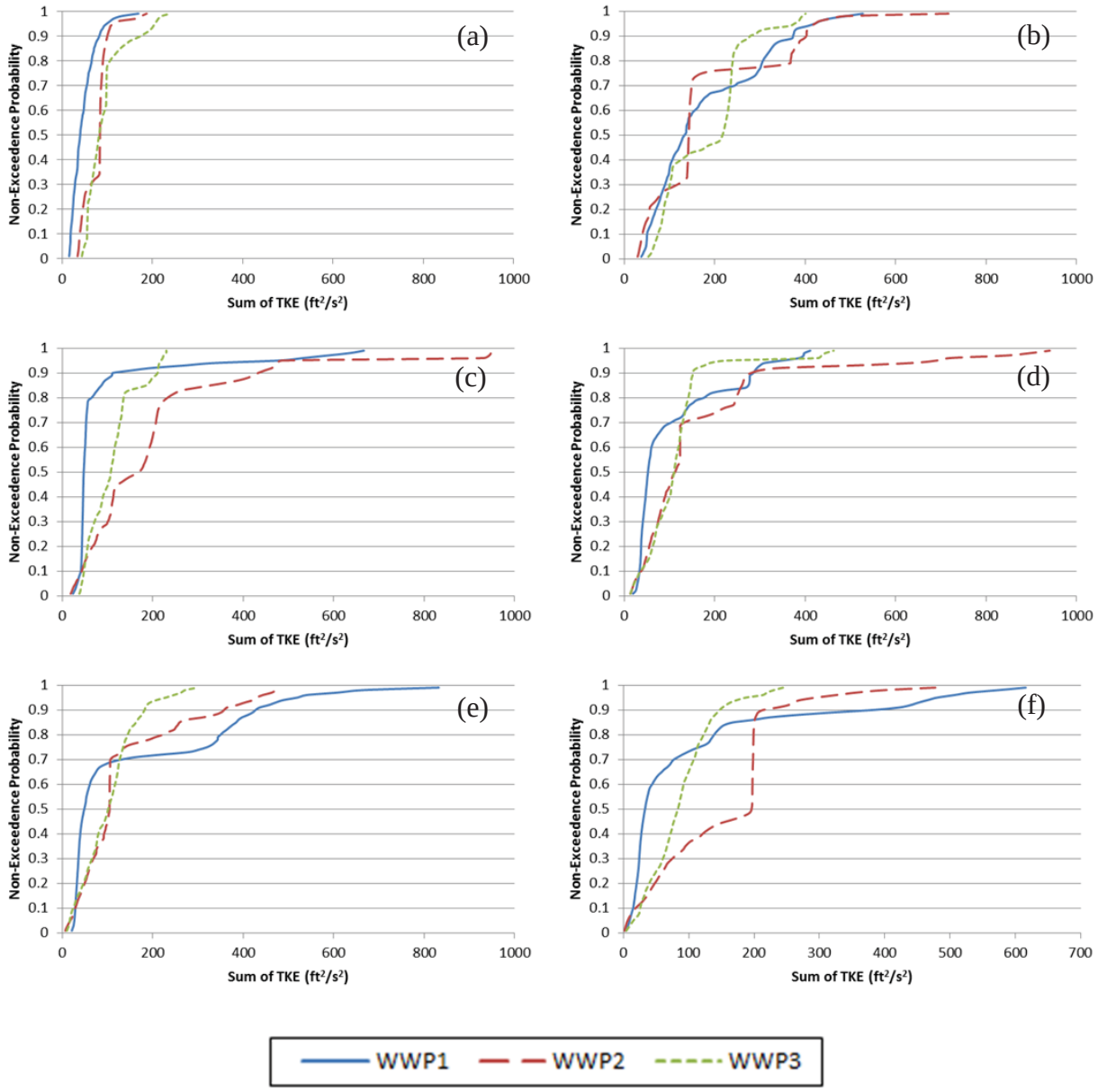

Figure 3.10: Non-exceedence probabilities for the sum of TKE along flow paths at each WWP structure for: (a) 15 cfs, (b) 30 cfs, (c) 60 cfs, (d) 100 cfs, (e) 150 cfs, and (f) 300 cfs.

3.2 Fish Passage

Fish passage success varies among WWP structures and size classes of fish (Figure 3.11). Passage success is greatest at WWP1 for fish 200 mm in length and smaller; however, passage success decreases as fish size increases at WWP1. WWP2 has the highest success rate for larger

fish. Additionally, there appears to be a positive linear relationship with passage success and fish size. At WWP3, passage success increases from 28 to 80 percent when fish length exceeds 300 mm. Different fractions of successful movements at each WWP structure occurred over different discharges (Figure 3.12). At 15 cfs, the largest fraction of successful movements occurred at WWP2. There is a mode of successful movements for all WWP structures at 30 cfs. Indeed, more than 80 percent of fish passage at WWP1 occurred at 30 cfs. At 60 cfs, a larger fraction of successful movements occurred at WWP3 compared to WWP1 and WWP2. As discharge increases from 100 to 300 cfs, the fraction of successful movements at each WWP greatly decreases.

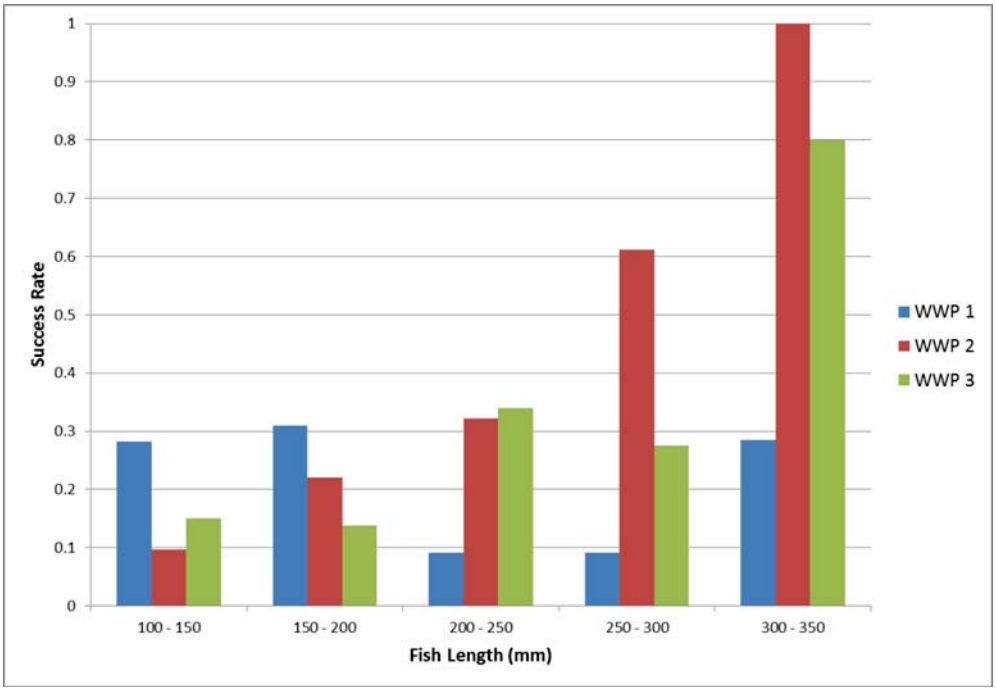

Figure 3.11: The fraction of observed fish by size class at each WWP structure that successfully passed that structure.

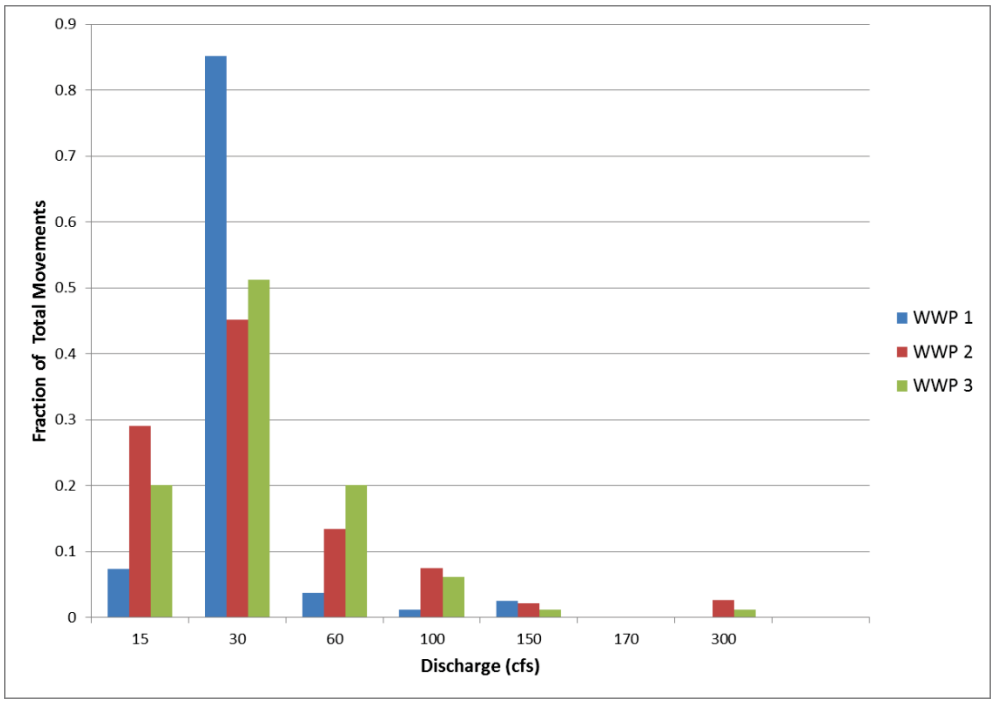

Figure 3.12: The fraction of successful movements occurring over the range of modeled discharges at each WWP structure.

3.3 Logistic Regression Analysis

Logistic regression analysis of hydraulic variables, i.e., percentile of cost tested individually with the maximum velocity ratio for 25 and 10 BL/s, the minimum depth criterion, the 50th percentile of the maximum vorticity, and the 50th percentile of the maximum TKE consistently indicated that maximum velocity ratio for 25 and 10 BL/s, and the minimum depth criterion were the best predictors of passage success across all WWP structures (Table 3.5). In contrast, the cost variable was a poor predictor of passage success (Appendix A). Removing the cost variable from the logistic regression model does not have a significant effect on the model fit.

Model parameter estimates indicate that passage success decreases with increases in the fractions of flow paths that exceed burst swimming ability and the minimum depth criterion

(Table 3.5). A unit change in the minimum depth criterion results in the greatest response in passage success compared to the maximum velocity ratio (odds ratio = 6.73×10^{-13}). The final model was highly significant ($p < 0.05$) with classification accuracies of 71.7 and 92.5 for successful and unsuccessful movements, respectively (Table 3.6).

Table 3.5: Logistic regression analysis for passage success across all WWP structures.

Predictor	β	SE β	χ^2	df	p	odds ratio (e^{β})
Constant	27.6948	2.2348	153.5700	1	<0.0001	–
Maximum Velocity Ratio (10 BL/s)	-2.4217	0.9061	7.1400	1	0.0075	0.0888
Maximum Velocity Ratio (25 BL/s)	-2.5155	0.5742	19.1900	1	<0.0001	0.0808
Minimum Depth Criterion	-28.0266	2.1821	164.9700	1	<0.0001	6.73E-13
Test			χ^2	**df**	**p**	
Overall model evaluation:						
Likelihood ratio test			271.7842	3	<0.0001	
Goodness-of-fit test			147.8854	3	0.1222	

Table 3.6: The observed and predicted frequencies for passage success across all WWP structures.

	Predicted		
Observed	**Pass**	**Did Not Pass**	**% Correct**
Pass	114	45	71.7%
Did Not Pass	37	458	92.5%
Overall % Correct			87.5%

Logistic regression analysis of each individual structure shows a significant influence of different hydraulic variables at each structure (Appendix A). Depth is statistically significant at WWP1, depth and the maximum velocity ratio for 25 BL/s are significant at WWP2, and depth and the maximum velocity ratio for 10 BL/s are significant at WWP3. The parameter estimates and odds ratio for the hydraulic variables at each individual structure show a decrease in the probability of success as the fraction of flow paths that exceed burst swimming ability increase (Table 3.7). The goodness-of-fit test at WWP1 indicates that more complex variables could be

added to the model ($p < 0.05$). Despite the results from the goodness-of-fit test at WWP1, the likelihood ratio test indicates that the models predict passage success with high accuracy ($p < 0.05$) (Table 3.7). Additionally, the model correctly predicted 76.14 percent of the observations. The logistic regression models accurately predicted 88.5 and 86 percent of the observations at WWP2 and WWP3, respectively (Table 3.8).

Table 3.7: Logistic regression analysis for passage success at each WWP structure.

	Predictor	β	SE β	χ^2	df	p	odds ratio (e^{β})
WWP1	Constant	31.9771	3.8436	69.2100	1	<0.0001	–
	Minimum Depth Criterion	-36.3190	4.2438	73.2400	1	<0.0001	1.69E-16
WWP2	Constant	29.7199	4.6198	41.3900	1	<0.0001	–
	Maximum Velocity Ratio (25 BL/s)	-4.8744	1.6846	8.3700	1	0.0038	7.64E-03
	Minimum Depth Criterion	-31.7426	4.6872	45.8600	1	<0.0001	1.64E-14
WWP3	Constant	26.8093	3.4570	60.1400	1	<0.0001	–
	Maximum Velocity Ratio (10 BL/s)	-3.2481	0.6892	22.2100	1	<0.0001	3.89E-02
	Minimum Depth Criterion	-26.2229	3.3716	60.4900	1	<0.0001	4.09E-12
	Test			χ^2	df	p	
WWP1	Overall model evaluation:						
	Likelihood ratio test			119.3776	1	<0.0001	
	Goodness-of-fit test			9.9828	1	0.0068	
WWP2	Overall model evaluation:						
	Likelihood ratio test			89.4292	2	<0.0001	
	Goodness-of-fit test			21.2561	2	0.9674	
WWP3	Overall model evaluation:						
	Likelihood ratio test			92.7136	2	<0.0001	
	Goodness-of-fit test			33.8460	2	0.1389	

Table 3.8: The observed and predicted frequencies for passage success at each individual WWP structure.

		Predicted		
	Observed	**Pass**	**Did Not Pass**	**% Correct**
WWP1	Pass	8	10	44.4%
	Did Not Pass	37	142	79.3%
	Overall % Correct			76.1%
WWP2	Pass	35	15	70.0%
	Did Not Pass	7	135	95.1%
	Overall % Correct			88.5%
WWP3	Pass	41	14	74.5%
	Did Not Pass	22	181	89.2%
	Overall % Correct			86.0%

Logistic regression analysis of the combined variable for the maximum velocity ratio and minimum depth criterion indicate a significant influence of the maximum velocity ratio for 25 BL/s and the minimum depth criterion; however, the maximum velocity ratio for 10 BL/s and the minimum depth criterion was not significant (Appendix A). The combined variable has a negative parameter estimate and odds ratio < 1, indicating that passage success decreases as the fraction of flow paths that exceed burst swimming ability (25 BL/s) or do not meet the minimum depth criterion increases (Table 3.9). The likelihood ratio test indicates that the model predicted passage success with high accuracy ($p < 0.05$); however, the goodness-of-fit test indicates that additional variables could be added to improve the model fit. The model accurately predicted 87.5 percent of the observations (Table 3.10).

Table 3.9: Logistic regression analysis for passage success across all WWP structures for the combined variable (maximum velocity ratio of 25 BL/s and the minimum depth criterion).

Predictor	β	SE β	χ^2	df	p	odds ratio (e^{β})
Constant	24.6694	2.0324	147.34	1	<0.0001	–
Maximum Velocity Ratio (25 BL/s) and the Minimum Depth Criterion	-27.2676	2.1608	159.24	1	<0.0001	1.44E-12
Test			χ^2	**df**	**p**	
Overall model evaluation:						
Likelihood ratio test			228.7675	1	<0.0001	
Goodness-of-fit test			81.9267	1	<0.0001	

Table 3.10: The observed and predicted frequencies for passage success across all WWP structures for the combined variable (maximum velocity ratio of 25 BL/s and the minimum depth criterion).

	Predicted		
Observed	**Pass**	**Did Not Pass**	**% Correct**
Pass	108	51	67.9%
Did Not Pass	31	464	93.7%
Overall % Correct			87.5%

Logistic regression analyses of each individual structure indicated a significant influence of the combined variable for the maximum velocity ratio of 25 BL/s and the minimum depth requirement. According to the odds ratios and parameter estimates, passage success decreases with an increase in the fraction of traces that exceed burst swimming ability (25 BL/s) or do not meet the minimum depth criterion increases (Table 3.11). The likelihood ratio test indicates that each model predicts passage success with high accuracy ($p < 0.05$) (Table 3.11). Additionally, the goodness-of-fit test at WWP2 and WWP3 indicates that the inclusion of additional variables would not improve the model fit ($p > 0.05$); however, the addition of more complex variables at WWP1 might improve the model fit ($p < 0.05$). The model accurately predicted passage success for 90.7, 87.5, and 85.7 percent of the observations at WWP1, WWP2, and WWP3, respectively (Table 3.12).

Table 3.11: Logistic regression analysis for passage success at each WWP structure for the combined variable (maximum velocity ratio of 25 BL/s and the minimum depth criterion).

	Predictor	β	SE β	χ^2	df	p	odds ratio (e^{β})
WWP1	Constant	45.0055	5.5986	64.62	1	<0.0001	–
	Maximum Velocity Ratio (25 BL/s) and the Minimum Depth Criterion	-49.7348	6.0592	67.37	1	<0.0001	2.51E-22
WWP2	Constant	24.8876	3.6464	46.58	1	<0.0001	–
	Maximum Velocity Ratio (25 BL/s) and the Minimum Depth Criterion	-27.0016	3.7769	51.11	1	<0.0001	1.88E-12
WWP3	Constant	20.4209	2.9188	48.95	1	<0.0001	–
	Maximum Velocity Ratio (10 BL/s) and the Minimum Depth Criterion	-22.6106	3.0498	54.96	1	<0.0001	1.51E-10

	Test	χ^2	df	p
WWP1	Overall model evaluation:			
	Likelihood ratio test	104.3809	1	<0.0001
	Goodness-of-fit test	38.4229	1	<0.0001
WWP2	Overall model evaluation:			
	Likelihood ratio test	80.308	1	<0.0001
	Goodness-of-fit test	13.6666	1	0.6235
WWP3	Overall model evaluation:			
	Likelihood ratio test	71.7071	1	<0.0001
	Goodness-of-fit test	0.0999	1	0.9513

Table 3.12: The observed and predicted frequencies for passage success at each individual WWP structure for the combined variable (maximum velocity ratio of 25 BL/s and the minimum depth criterion).

		Predicted		
	Observed	Pass	Did Not Pass	% Correct
WWP1	Pass	43	11	79.6%
	Did Not Pass	8	142	94.7%
	Overall % Correct			90.7%
WWP2	Pass	33	17	66.0%
	Did Not Pass	7	135	95.1%
	Overall % Correct			87.5%
WWP3	Pass	34	21	61.8%
	Did Not Pass	16	187	92.1%
	Overall % Correct			85.7%

CHAPTER 4 DISCUSSION

The methods used in this study provide a novel and powerful approach to evaluate fish passage at hydraulic structures. Describing the hydraulic conditions along potential fish movement paths continuously quantifies important flow features at a scale meaningful to a fish. The logistic regression analyses indicate that the maximum velocity ratio for burst swimming abilities of 25 and 10 BL/s and the minimum depth criterion accurately predict passage success for over 87 percent of observed trout. Additionally, the model accurately predicted over 92 percent of the observations of no movement. The fraction of available flow paths that exceed a fish's burst swimming ability or do not provide adequate depth had a negative influence on passage success. This strongly suggests that both depth and velocity are contributing to the suppression of movement of upstream migrating salmonids. These results contrast with a previous study that did not find velocity to have an evident effect on passage success (Fox, 2013). This contradiction is likely the result of the difference in scale over which velocities were quantified. Fox (2013) calculated cross-sectional velocity quantiles within the chute of WWP structures not accounting for discontinuities in acceptable velocities along a movement path.

Logistic regression analysis indicates a significant influence of the combined variable for the maximum velocity ratio (25 BL/s) and the minimum depth criterion across all WWP structures and at each individual WWP structure. This underscores the importance of jointly considering depth and velocity as barriers to upstream migration. Additionally, combining velocity and depth into a single variable allows for a simplified, but highly accurate, statistical analysis. Quantifying a single variable provides a means to assess passage success with fewer observed movements. This could have implications for future projects where time and cost are limiting factors.

Although the combined variable accurately captures the effects of velocity and depth, additional analyses of the variation in statistically significant hydraulic variables among WWP structures highlights unique hydraulic characteristics at each WWP structure that affect passage success differently. Depth is the primary limiting factor contributing to the suppression of movement at WWP1, while both velocity and depth have significant influences at WWP2 and WWP3. The evaluation of the maximum velocity ratio, depth, and their joint influence on passage success by size class and discharge emphasizes the importance of site-specific characterization of subtle differences in structure design. However, depth has lowest odds ratio in all logistic regression analyses suggesting it has the strongest effect on passage success.

At lower discharges, continuous passage routes across WWP1 are only accessible through narrow chutes (< 1 ft) flowing in between boulders that may not provide adequate depth or flow area for larger fish, but do provide lower velocities accessible to smaller fish. This is confirmed through logistic regression, the maximum velocity ratio and depth variables, and observed passage success by size class. Depth presents the greatest challenge across discharges at WWP1, and examining the maximum velocity ratio for burst swimming abilities of 10 BL/s and depth concurrently indicates that WWP1 provides the most available flow paths for smaller fish. Depth is the only statistically significant variable influencing passage success at WWP1, and higher success rates are observed for smaller fish compared to larger fish at WWP1.

WWP2 constricts the flow to the center of the chute at lower discharges and forces fish to traverse shallow flow depths characterized by the highest velocities. This is reflected in the lack of available flow paths exceeding 0.6 ft at 15 cfs and the fraction of flow paths that exceed burst swimming ability for 25 BL/s at 30 cfs. At 30 cfs, the fraction of accessible flow paths is limited and similar among size classes for a 175- to 300-mm fish indicating concentrated flow. When

observing higher discharges and the fraction of available flow paths for 10 BL/s, there is a positive linear increase in the amount of available flow paths with fish size that is reflective of a linear increase in passage success. Further, logistic regression confirms depth and velocity as significant influences on passage success at WWP2. As discharge increases, flow spills over the wing walls and a small zone adjacent to the left bank provides lower velocities.

At WWP3, recirculation zones exist adjacent to the main velocity jet. At lower flows these low-velocity zones may not provide adequate flow depth, forcing fish to pass through the main velocity jet. These flow patterns are confirmed by examining the aggregate effect of the maximum velocity ratio for 10 BL/s and depth. Depth appears to prevent passage at 15 cfs, while passage is accessible to larger fish as discharge increases to 30 cfs indicating velocity as the limiting factor. Fish movement data show a similar threshold of increased passage success for larger fish at WWP3. However, as discharge increases, water spills over the wing walls, flow depths increase adjacent to the main velocity jet, and more flow paths become available to larger fish. Logistic regression verifies depth and velocity as significant influences on passage success at WWP3.

It is interesting that the maximum velocity ratios for burst swimming abilities of 10 and 25 BL/s are both statistically significant. Fish naturally vary in their physical capabilities much like humans (Williams *et al*., 2012). Thus, a variation in physical capabilities among fish is likely illustrated through the inclusion of the maximum velocity ratio for burst swimming abilities of 10 and 25 BL/s. This is consistent with a previous study examining passage success through fishways, where not all fish were able to pass a structure equally well (Caudill *et al*., 2007). Additionally, burst swimming abilities of 10 and 25 BL/s agree with the different findings of previous laboratory studies (Beamish, 1978; Peake *et al*., 1997; Castro-Santos *et al*.,

2013). Further, a mixed population of hatchery fish and naturally producing fish supports the inclusion of different burst swimming abilities. It has been shown that hatchery rearing can alter the behavior and swimming ability of fish (Duthie, 1987; Peake *et al*., 1997). The inclusion of the maximum velocity ratio for different burst swimming abilities at individual structures could also indicate the influence of additional hydraulic variables, such as depth or turbulence, to reduce a fish's swimming ability.

The goodness-of-fit test at WWP1 shows that more complex variables could improve the model fit. This suggests that additional variables to depth could be contributing to the suppression of movement at WWP1. A study examining the effects of turbulence on passage success in three different pool-type fishways found that the fishway with the highest turbulence had the worst passage success, but passed smaller fish better than the other configurations (Silva *et al*., 2012). Similarly, WWP1 has the worst overall passage success; however, smaller fish experience higher success rates at WWP1 compared to larger fish. WWP1 is also characterized by the highest magnitudes and larger distribution of the maximum vorticity along flow paths at discharges when the majority of the movements occurred. This suggests that turbulence could be an additional factor affecting passage success at WWP1.

The fact that our models did not identify turbulence as a significant influence could be an issue of scale. It has been suggested that the intensity, periodicity, orientation, and scale (IPOS) of turbulence should be considered in conjunction when relating turbulence to fish swimming abilities (Lacey *et al*., 2012). The magnitude or intensity of vorticity and TKE do not account for the spatial scale at which fish experience turbulent eddies relative to body length. Turbulent eddies that are small compared with the fish scale lack momentum required to negatively affect a fish, and in some cases assist in forward movement (Haro *et al*., 2004, Hinch and Rand, 2000;

Lacey *et al*., 2012). Turbulent eddies with a diameter close to the length of a fish can pose stability challenges and reduce a fish's swimming ability (Lupandin, 2005; Pavlov *et al*., 2000; Tritico and Cotel, 2010). However, examining these relationships remains difficult without direct observations of flow/fish interactions and established thresholds of the effects of turbulence on fish swimming abilities.

The cumulative effects of velocity a fish experiences while crossing a structure have the potential to influence passage success. Studies have shown that as the swim speed of a fish increases the time to fatigue decreases (Bainbridge, 1960; Peake *et al*., 1997). The difference in the lengths of the flow volumes is a direct result of differences in the length of the hydraulic jump at each structure. The length of the hydraulic jump is greatest at WWP3, resulting in greater distances of supercritical flow and higher velocities. Consequently, WWP3 is characterized by the highest 50^{th} percentile of cost with the exception of 60 cfs. However, similar costs exist at WWP2 and WWP3 at lower flows. As discharge increases, lower velocities along the channel margins at WWP3 provide similar costs between WWP3 and WWP2 below the 50^{th} percentile. Considering a fish chooses the least cost path (McElroy *et al*., 2012) through a structure, it is unlikely that an exhaustive swimming barrier will exist. Logistic regression analysis does not indicate a negative effect of cost on passage success; however, visual observations of failed attempts will reveal direct relationships on passage success and velocity as an exhaustive swimming barrier.

Passage success across barriers to migration is a function of the behavior and physiological limits of a fish (Castro-Santos *et al*., 2013). This study examines hydraulic conditions as physiological barriers to migration and does not take into account fish behavior. Accessible movement paths might exist at a structure. However, a fish might feel the cumulative

effects of fatigue or lack motivation or willingness after several failed attempts to locate accessible movement paths (Castro-Santos *et al*., 2013). It is important to consider the timing of fish migrations and other life-cycle processes. Although higher discharges provide a higher fraction of accessible flow paths for fish, discharges at 15 to 60 cfs occur much more frequently throughout the year at the study site.

Despite the remaining uncertainties in additional factors that might be contributing to the suppression of movement, management guidance and design recommendations can be provided based on the strong relationship of passage success with velocity and depth. Care should be taken to ensure that velocity and depth requirements are met continuously along likely fish movement paths. Multiple field studies indicate that fish exploit boundary layers created by objects in the flow field (Fausch, 1993; Nestler *et al*., 2008). Interstitial spaces within the center of the chute may provide zones of lower velocity for smaller fish. Increasing the size range of the interstitial spaces to at least the body depth of largest fish likely encountered may provide adequate flow depth and lower velocities to accommodate a broader size class of fish size. Continuous low-velocity zones along the margins of the chute with adequate flow depth should be provided, allowing fish to avoid the main velocity jet. Low-velocity zones along the channel margins can be achieved by allowing water to spill over the wing walls at all discharges. If the wing walls are not grouted they act as roughness elements providing flow refugia for fish. Large eddies that recirculate back into the chute at all discharges can provide additional low-velocity zones as seen at higher discharges at WWP3. These low-velocity recirculation zones should come up the sides of the main velocity jet as far as possible.

Quantifying hydraulic conditions along potential fish movement paths provides a novel and powerful approach to mechanistically evaluate the effects of hydraulics on fish passage over

a wide range of hydraulic structure types. When assessing WWP designs, it is important to describe the hydraulic conditions at scales that fish experience them. Simply averaging the hydraulic conditions over large spatial scales or evaluating point measurements do not take into account the continuous complexity of the flow field along a fish's movement path. It is also important to consider the interaction between multiple hydraulic variables such as depth and velocity to ensure all conditions are met for successful passage.

The results of this study are potentially limited in their transferability to assessing passage success of salmonids at WWPs of similar size, design type, and hydrologic regime. Similar hydraulic analyses can provide information on the effects that velocity and depth might have on passage success at additional WWPs. Evaluating additional WWPs is highly recommended to determine the range of hydraulic conditions that fish are required to pass. Further, assessing passage success of non-salmonid fishes with different swimming abilities or behaviors could highlight the need for lower velocity zones or higher topographic diversity within WWP chutes. A more in-depth analysis of turbulence incorporating flow/fish interactions could reveal new thresholds and additional factors that affect passage success. Additionally visual observations of successful and failed attempts of individual fish will allow for a more-detailed comparison of the hydraulic conditions that effect passage success and shed light on behavioral limitations.

CHAPTER 5 CONCLUSIONS

This study used the results from a 3-D CFD model to provide a continuous and spatially explicit description of the hydraulic conditions along potential fish movement paths and examine their influence on fish passage at an actual WWP on the St. Vrain River in Lyons, Colorado. Quantifying the hydraulic conditions in this manner captured important and unique hydraulic characteristics at each WWP, and described velocity and depth throughout the flow field at a scale meaningful to a fish. A comparison of velocity and depth relative to a fish's swimming ability was reflective of the variation in passage success among WWP structures and size classes of fish. Logistic regression indicated a significant influence of velocity and depth on passage success, and accurately predicted 87 percent of individual fish observations. Specific combinations of depth and velocity were statistically significant at individual WWP structures highlighting the effects of unique hydraulic conditions at each WWP on passage success. The results indicate that additional variables such as turbulence might also be contributing to the suppression of movement. Further research is needed to examine the range of hydraulic conditions at existing WWPs and the effects of WWPs on native fishes with lesser swimming abilities. Additionally, studies involving flow/fish interactions are needed to evaluate fish behavior in response to hydraulic conditions and define turbulence at a scale relative to fish size. Similar hydraulic analyses coupled with fish movement data can be utilized to evaluate the effects of hydraulic conditions on passage success at other types and sizes of WWPs. This study lays the groundwork for a novel and powerful approach to mechanistically evaluate the effects of hydraulic structures on fish passage. Further, the results of this study can serve as a reference for managers and policy makers, provide design guidance for future WWPs, and be used to evaluate existing WWPs of similar size, design type, and hydrologic regime.

BIBLIOGRAPHY

Bainbridge, R. (1960). Speed and stamina in three fish. *Journal of Experimental Biology*, **37**(1):129–153.

Baxter, C. V., K. D. Fausch, M. Murakami, and P. L. Chapman (2004). Fish invasion restructures stream and forest food webs by interrupting reciprocal prey subsidies. *Ecology*, **85**:2656–2663, DOI: 10.1890/04-138.

Beamish, F. W. H. (1978). Swimming capacity. Pages 101-189 *in* W. S. Hoar and D. J. Randall (Eds.): Fish Physiology, Vol. VII, Locomotion, Academic Press, London, UK.

Beechie, T. J., D. A. Sear, J. D. Olden, G. R. Pess, J. M. Buffington, H. Moir, P. Roni, and M. M. H. Pollock (2010). Process-based principles for restoring river ecosystems. *BioScience*, **60**(3):209–222, URL: http://www.jstor.org/stable/10.1525/bio.2010.60.3.7.

Bunt, C. M., T. Castro-Santos, and A. Haro (2012). Performance of fish passage structures at upstream barriers to migration. *River Research and Applications*, **28**(4):457–478, DOI: 10.1002/rra.1565.

Caudill, C. C., W. R. Daigle, M. L. Keefer, C. T. Boggs, M. A. Jepson, B. J. Burke, R. W. Zabel, T. C. Bjornn, and C. A. Peery (2007). Slow dam passage in adult Columbia River salmonids associated with unsuccessful migration: Delayed negative effects of passage obstacles or condition-dependent mortality? *Canadian Journal of Fisheries and Aquatic Sciences*, **64**(7):979–995, DOI: 10.1139/F07-065.

Castro-Santos, T., A. Cotel, and P. Webb (2009). Fishway evaluations for better bioengineering: An integrative approach. Pages 557–575 *in* A. Haro, K. L. Smith, R. A. Rulifson, C. M. Moffitt, R. J. Klauda, M. J. Dadswell, R. A. Cunjak, J. E. Cooper, K. L. Beal, and T. S.

Avery (Eds.), Challenges for Diadromous Fishes in a Dynamic Global Environment, Conference Proceedings.

Castro-Santos, T., F. J. Sanz-Ronda, and J. Ruiz-Legazpi (2013). Breaking the speed limit—comparative sprinting performance of brook trout (*Salvelinus fontinalis*) and brown trout (*Salmo trutta*). *Canadian Journal of Fisheries and Aquatic Sciences*, **70**(2):280–293, DOI: 10.1139/cjfas-2012-0186.

Chow, V. T. (1959). Open Channel Hydraulics. McGraw-Hill, New York, NY.

Computational Engineering International, Inc. (2013). EnSight User Manual for Version 10.1. Computational Engineering International, Inc., Apex, NC.

Cotel, A. J., and P. W. Webb (2012). The challenge of understanding and quantifying fish responses to turbulence-dominated physical environments. Pages 15–33 *in* S. Childress, A. Hosoi, W. W. Schultz, and J. Wang (Eds.): Natural Locomotion in Fluids and on Surfaces, Springer Science+Business Media New York.

Crowder, D. W., and P. Diplas (2000). Using two-dimensional hydrodynamic models at scales of ecological importance. *Journal of Hydrology*, **230**(3-4):172–191, DOI: 10.1016/S0022-1694(00)00177-3.

Crowder, D. W., and P. Diplas (2002). Vorticity and circulation: Spatial metrics for evaluating flow complexity in stream habitats. *Canadian Journal of Fisheries and Aquatic Sciences*, **59**(4):633–645, DOI: 10.1139/f02-037.

Crowder, D. W., and P. Diplas (2006). Applying spatial hydraulic principles to quantify stream habitat. *River Research and Applications*, **22**(1):79–89, DOI: 10.1002/rra.893.

Dane, B. G. (1978). A Review and Resolution of Fish Passage Problems at Culvert Sites in British Columbia. Fisheries & Marine Service Technical Report No. 810, Department of Fisheries and Environment, Vancouver, BC, September, 126 p.

Dudley, R. K., and S. P. Platania (2007). Flow regulation and fragmentation imperil pelagic-spawning riverine fishes. *Ecological Applications*, **17**(7):2074–2086.

Duthie, G. G. (1987). Observations of poor swimming performance among hatchery-reared rainbow trout, *Salmo gairdneri*. *Environmental Biology of Fishes*, **18**(4):309–311, DOI: 10.1007/BF00004884.

Fagan, W. F. (2002). Connectivity, fragmentation, and extinction risk in dendritic metapopulations. *Ecology,* **83**(12):3243–3249, DOI: 10.1890/0012-9658(2002)083[3243: CFAERI]2.0.CO;2.

Fausch, K. D. (1993). Experimental analysis of microhabitat selection by juvenile steelhead (*Oncorhynchus mykiss*) and coho salmon (*O. kisutch*) in a British Columbia stream. *Canadian Journal of Fisheries and Aquatic Sciences*, **50**(6):1198–1207, DOI: 10.1139/f93-136.

Fausch, K. D., C. E. Torgersen, C. V. Baxter, and H. W. Li (2002). Landscapes to riverscapes: Bridging the gap between research and conservation of stream fishes. *BioScience*, **52**(6):483–498.

Fitch, G. M. (1995). Nonanadromous fish passage in highway culverts. Final Report No. VTRC 96-R6, Virginia Transportation Research Council, Charlottesville, VA.

FLOW Science (2009). FLOW-3D v9.4 User Manual. FLOW Science, Santa Fe, NM.

Fox, B. (2013). Eco-Hydraulic Evaluation of Whitewater Parks as Fish Passage Barriers. Masters Thesis, Colorado State University, Department of Civil and Environmental Engineering, Fort Collins, CO.

Frissell, C. A., W. J. Liss, C. E. Warren, and M. D. Hurley (1986). A hierarchical framework for stream habitat classification: Viewing streams in a watershed context. *Environmental Management*, **10**(2):199–214, DOI: 10.1007/BF01867358.

Frissell, C. A., N. L. Poff, and M. E. Jensen (2001). Assessment of biotic patterns in freshwater ecosystems. Pages 390–403 *in* M. E. Jensen and P. S. Bourgeron (Eds.): A Guidebook for Integrated Ecological Assessments, Springer Science+Business Media New York, 536 p.

Fullerton, A. H., K. M. Burnett, E. A. Steel, R. L. Flitcroft, G. R. Pess, B. E. Feist, C. E. Torgersen, D. J. Miller, and B. L. Sanderson (2010). Hydrological connectivity for riverine fish: Measurement challenges and research opportunities. *Freshwater Biology*, **55**(11):2215–2237, DOI: 10.1111/j.1365-2427.2010.02448.x.

Goodwin, R. A., J. M. Nestler, J. J. Anderson, L. J. Weber, and D. P. Loucks (2006). Forecasting 3-D fish movement behavior using a Eulerian–Lagrangian–agent method (ELAM). *Ecological Modelling*, **192**(1-2):197–223, DOI: 10.1016/j.ecolmodel.2005.08.004.

Hagenstad, M., J. Henderson, R. S. Raucher, and J. Whitcomb (2000). Preliminary Evaluation of the Beneficial Value of Waters Diverted in the Clear Creek Whitewater Park in the City of Golden. Unpublished Project Report prepared by Stratus Consulting Inc., Boulder, CO, 15 p., URL: http://www.boaterparks.com/Gold_economicimpact.pdf.

Haro, A., T. Castro-Santos, J. Noreika, and M. Odeh (2004). Swimming performance of upstream migrant fishes in open-channel flow: A new approach to predicting passage through velocity barriers. *Canadian Journal of Fisheries and Aquatic Sciences*, **61**(9):1590–1601, DOI: 10.1139/F04.

Hinch, S. G., and P. S. Rand (2000). Optimal swimming speeds and forward-assisted propulsion: Energy-conserving behaviours of upriver-migrating adult salmon. *Canadian Journal of Fisheries and Aquatic Sciences*, **57**(12):2470–2478, DOI: 10.1139/f00-238.

Hotchkiss, R. H., and C. M. Frei (2007). Design for Fish Passage at Roadway-stream Crossings: Synthesis Report. Publication No. FHWA-HIF-07-033, U. S. Department of Transportation, Federal Highway Administration, McLean, VA, June, 280 p.

Katopodis, C. (2005). Developing a toolkit for fish passage, ecological flow management and fish habitat works. *Journal of Hydraulic Research*, **43**(5):451–467, DOI: 10.1080/00221680509500144.

Kilgore, R. T., B. S. Bergendahl, and R. H. Hotchkiss (2010). Culvert Design for Aquatic Organism Passage. Hydraulic Engineering Circular No. 26 (HEC-26), Publication No. FHWA-HIF-11-008, U. S. Department of Transportation, Federal Highway Administration, October, 234 p.

Kolden, E. (2013). Modeling in a Three-dimensional World: Whitewater Park Hydraulics and Their Impact on Aquatic Habitat in Colorado. Masters Thesis, Colorado State University, Department of Civil and Environmental Engineering, Fort Collins, CO.

Lacey, R. W., V. S. Neary, J. C. Liao, E. C. Enders, and H. M. Tritico (2012). The IPOS framework: Linking fish swimming performance in altered flows from laboratory experiments to rivers. *River Research and Applications*, **28**(4):429–443, DOI: 10.1002/rra.1584.

Liao, J. C. (2007). A review of fish swimming mechanics and behaviour in altered flows. *Philosophical Transactions of the Royal Society B: Biological Sciences*, 362(1487):1973–1993, DOI: 10.1098/rstb.2007.2082.

Lupandin, A. I. (2005). Effect of flow turbulence on swimming speed of fish. *Biology Bulletin*, **32**(5):461–466, DOI: 10.1007/s10525-005-0125-z.

McElroy, B., A. DeLonay, and R. Jacobson (2012). Optimum swimming pathways of fish spawning migrations in rivers. *Ecology*, **93**(1):29–34, DOI: 10.1890/11-1082.1.

McGrath, C. C. (2003). Potential Effects of Whitewater Parks on In-Stream Trout Habitat. Unpublished Project Report prepared for Recreational Engineering and Planning, Inc., Boulder, CO, 12 p., URL: http://www.boaterparks.com/Web%20fish%20report.pdf.

National Oceanic and Atmospheric Administration (NOAA) (2001). Guidelines for Salmonid Passage at Stream Crossings. NOAA, National Marine Fisheries Service, Southwest Region, September.

Nestler, J. M., R. A. Goodwin, D. L. Smith, J. J. Anderson, and S. Li (2008). Optimum fish passage and guidance designs are based in the hydrogeomorphology of natural rivers. *River Research and Applications*, **24**(2):148–168, DOI: 10.1002/rra.1056.

Nestler, J. M., P. S. Pompeu, R. A. Goodwin, D. L. Smith, L. G. M. Silva, C. R. M. Baigún, and N. O. Oldani (2012). The river machine: A template for fish movement and habitat, fluvial geomorphology, fluid dynamics and biogeochemical cycling. *River Research and Applications*, **28**(4):490–503, DOI: 10.1002/rra.1567.

Nilsson, C., C. A. Reidy, M. Dynesius, and C. Revenga (2005). Fragmentation and flow regulation of the world's large river systems. *Science*, **308**(5720):405–408, DOI: 10.1126/science.1107887.

Pavlov, D. S., A. I. Lupandin, and M. A. Skorobogatov (2000). The effects of flow turbulence on the behavior and distribution of fish. *Journal of Ichthyology*, **20**:S232–S261.

Peake, S., R. S. McKinley, and D. A. Scruton (1997). Swimming performance of various freshwater Newfoundland salmonids relative to habitat selection and fishway design. *Journal of Fish Biology*, **51**(4):710–723, DOI: 10.1111/j.1095-8649.1997.tb01993.x.

Perkin, J. S., and K. B. Gido (2012). Fragmentation alters stream fish community structure in dendritic ecological networks. *Ecological Applications*, **22**(8):2176–2187.

Poff, N. L., J. D. Allan, M. B. Bain, J. R. Karr, K. L. Prestegaard, B. Richter, R. Sparks, and J. Stromberg (1997). The natural flow regime: A new paradigm for riverine conservation and restoration. *BioScience*, **47**:769–784.

SAS Institute Inc. (2013). Using JMP® 11. SAS Institute Inc., Cary, NC.

Schlosser, I. J., and P. L. Angermeier (1995). Spatial variation in demographic processes of lotic fishes: Conceptual models, empirical evidence, and implications for conservation. *American Fisheries Society Symposium*, **17**:392–401.

Silva, A. T., C. Katopodis, J. M. Santos, M. T. Ferreira, and A. N. Pinheiro (2012). Cyprinid swimming behaviour in response to turbulent flow. *Ecological Engineering*, **44**:314–328, DOI: 10.1016/j.ecoleng.2012.04.015.

Thorp, J. H., M. Thoms, and M. D. Delong (2006). The riverine ecosystem synthesis: Biocomplexity in river networks across space and time. *River Research and Applications*, **22**(2):123–147, DOI: 10.1002/rra.901.

Tritico, H. M., and A. J. Cotel (2010). The effects of turbulent eddies on the stability and critical swimming speed of creek chub (*Semotilus atromaculatus*). *The Journal of Experimental Biology*, **213**(13):2284–2293, DOI: 10.1242/jeb.041806.

Walters, D. M., R. E. Zuellig, H. J. Crockett, J. F. Bruce, P. M. Lukacs, and R. M. Fitzpatrick (2014). Barriers impede upstream spawning migration of flathead chub. *Transactions of the American Fisheries Society*, **143**(1):17–25, DOI: 10.1080/00028487.2013.824921.

Webb, P. W. (1975). Hydrodynamics and Energetics of Fish Propulsion. Bulletin 190, Bulletin of the Fisheries Research Board of Canada, Ottawa, Canada, 160 p.

Webb, P. W. (1998). Swimming. Pages 3–24 *in* D. H. Evans (Ed.): The Physiology of Fishes, Second Edition, CRC Press, Washington, DC.

Williams, J. G., G. Armstrong, C. Katopodis, M. Larinier, and F. Travade (2012). Thinking like a fish: A key ingredient for development of effective fish passage facilities at river obstructions. *River Research and Applications*, **28**(4):407–417, DOI: 10.1002/rra.1551.

Wohl, E., P. L. Angermeier, B. P. Bledsoe, G. M. Kondolf, L. MacDonnell, D. M. Merritt, M. A. Palmer, N. L. Poff, and D. Tarboton (2005). River restoration. *Water Resources Research*, **41**:W10301, DOI: 10.1029/2005WR003985.

APPENDIX A LOGISTIC REGRESSION ANALYSIS

Correlations

	25BLS	10BLS	20BLS	5 Cost	16 Cost	50 Cost	84 Cost	95 Cost	sum vort	max vort	sum tke	max tke	Depth
25BLS	1.0000	0.1136	0.6069	-0.0392	0.0337	-0.0098	0.1169	0.0630	-0.1714	-0.2502	0.1153	0.3198	-0.3173
10BLS	0.1136	1.0000	0.1796	0.0291	0.0435	0.0244	0.0296	-0.0182	0.0460	-0.0140	0.0880	-0.0035	-0.0672
20BLS	0.6069	0.1796	1.0000	0.0001	0.0353	-0.0249	0.0220	-0.0749	-0.1411	-0.2028	0.0706	0.0561	-0.1593
5 Cost	-0.0392	0.0291	0.0001	1.0000	0.9805	0.9626	0.8837	0.8102	0.4078	0.3404	0.5673	0.4437	0.1618
16 Cost	0.0337	0.0435	0.0353	0.9805	1.0000	0.9764	0.9326	0.8455	0.4158	0.2687	0.6175	0.5088	0.0323
50 Cost	-0.0098	0.0244	-0.0249	0.9626	0.9764	1.0000	0.9617	0.9115	0.5270	0.4244	0.6806	0.5729	-0.0584
84 Cost	0.1169	0.0296	0.0220	0.8837	0.9326	0.9617	1.0000	0.9572	0.5002	0.3468	0.7258	0.7326	-0.2395
95 Cost	0.0630	-0.0182	-0.0749	0.8102	0.8455	0.9115	0.9572	1.0000	0.4704	0.4152	0.6238	0.8013	-0.1991
sum vort	-0.1714	0.0460	-0.1411	0.4078	0.4158	0.5270	0.5002	0.4704	1.0000	0.8401	0.8665	0.3399	-0.3693
max vort	-0.2502	-0.0140	-0.2028	0.3404	0.2687	0.4244	0.3468	0.4152	0.8401	1.0000	0.6403	0.3207	-0.1842
sum tke	0.1153	0.0880	0.0706	0.5673	0.6175	0.6806	0.7258	0.6238	0.8665	0.6403	1.0000	0.5871	-0.5293
max tke	0.3198	-0.0035	0.0561	0.4437	0.5088	0.5729	0.7326	0.8013	0.3399	0.3207	0.5871	1.0000	-0.4301
Depth	-0.3173	-0.0672	-0.1593	0.1618	0.0323	-0.0584	-0.2395	-0.1991	-0.3693	-0.1842	-0.5293	-0.4301	1.0000

Figure A.1: Bivariate analysis of each individual variable.

Current Estimates

Lock	Entered	Parameter	Estimate	nDF	Wald/Score ChiSq	"Sig Prob"
☑	☑	Intercept[0]	27.0967458	1	0	1
☐	☑	Maximum Velocity Ratio (25BL/s)	-2.6609068	1	4.086871	0.04322
☐	☑	Maximum Velocity Ratio (10BL/s)	-2.5683701	1	21.25984	4.01e-6
☐	☑	5th Percentile Cost	0.00193729	1	8.496178	0.00356
☐	☑	Minimum Depth Requirement	-28.326302	1	69.73938	6.8e-17
☐	☐	Maximum Vorticity	0	1	0.029632	0.86333
☐	☐	Maximum TKE	0	1	0.854243	0.35535

Whole Model Test

Model	-LogLikelihood	DF	ChiSquare	Prob>ChiSq
Difference	143.72304	4	287.4461	<.0001*
Full	219.01731			
Reduced	362.74035			

RSquare (U)	0.3962
AICc	448.127
BIC	470.45
Observations (or Sum Wgts)	654

Measure	Training	Definition
Entropy RSquare	0.3962	1-Loglike(model)/Loglike(0)
Generalized RSquare	0.5307	(1-(L(0)/L(model))^(2/n))/(1-L(0)^(2/n))
Mean -Log p	0.3349	∑ -Log(ρ[j])/n
RMSE	0.3133	√ ∑(y[j]-ρ[j])²/n
Mean Abs Dev	0.1961	∑ |y[j]-ρ[j]|/n
Misclassification Rate	0.1208	∑ (ρ[j]≠ρMax)/n
N	654	n

Unit Odds Ratios

Per unit change in regressor

Term	Odds Ratio	Lower 95%	Upper 95%	Reciprocal
Maximum Velocity Ratio (25BL/s)	0.069885	0.010338	0.385431	14.309259
Maximum Velocity Ratio (10BL/s)	0.07666	0.025588	0.235747	13.044545
5th Percentile Cost	1.001939	1.000959	1.002974	0.9980646
Minimum Depth Requirement	4.99e-13	6.71e-15	2.85e-11	2.004e+12

(a) 5th percentile of cost

Figure A.2: Preliminary variables selected by stepwise forward regression and their inclusion in logistic regression for: (a) 5th percentile of cost, (b) 16th percentile of cost, (c) 50th percentile of cost, (d) 84th percentile of cost, and (e) 95th percentile of cost.

Current Estimates

Lock	Entered	Parameter	Estimate	nDF	Wald/Score ChiSq	"Sig Prob"
☑	☑	Intercept[0]	26.5971378	1	0	1
☐	☑	Maximum Velocity Ratio (25BL/s)	-2.7422313	1	3.715558	0.05391
☐	☑	Maximum Velocity Ratio (10BL/s)	-2.5651149	1	20.3414	6.48e-6
☐	☑	16th Percentile	0.001706	1	5.651824	0.01744
☐	☐	Maximum Vorticity	0	1	0.775594	0.37849
☐	☐	Maximum TKE	0	1	0.272142	0.6019
☐	☑	Minimum Depth Requirement	-27.762903	1	73.56606	9.7e-18

Whole Model Test

Model	-LogLikelihood	DF	ChiSquare	Prob>ChiSq
Difference	142.23580	4	284.4716	<.0001*
Full	220.50455			
Reduced	362.74035			

RSquare (U)	0.3921
AICc	451.102
BIC	473.425
Observations (or Sum Wgts)	654

Measure	Training	Definition
Entropy RSquare	0.3921	1-Loglike(model)/Loglike(0)
Generalized RSquare	0.5263	(1-(L(0)/L(model))^(2/n))/(1-L(0)^(2/n))
Mean -Log p	0.3372	∑ -Log(ρ[j])/n
RMSE	0.3144	√ ∑(y[j]-ρ[j])²/n
Mean Abs Dev	0.1977	∑ |y[j]-ρ[j]|/n
Misclassification Rate	0.1208	∑ (ρ[j]≠ρMax)/n
N	654	n

Unit Odds Ratios

Per unit change in regressor

Term	Odds Ratio	Lower 95%	Upper 95%	Reciprocal
Maximum Velocity Ratio (25BL/s)	0.064426	0.009286	0.358399	15.521579
Maximum Velocity Ratio (10BL/s)	0.07691	0.025613	0.237481	13.002151
16th Percentile	1.001707	1.000757	1.002698	0.9982955
Minimum Depth Requirement	8.76e-13	1.22e-14	4.85e-11	1.141e+12

(b) 16th percentile of cost

Figure A.2 (continued)

Current Estimates

Lock	Entered	Parameter	Estimate	nDF	Wald/Score ChiSq	"Sig Prob"
☑	☑	Intercept[0]	25.8096838	1	0	1
☐	☑	Maximum Velocity Ratio (25BL/s)	-2.5231612	1	3.709324	0.05411
☐	☑	Maximum Velocity Ratio (10BL/s)	-2.5201584	1	19.9571	7.92e-6
☐	☑	50th Percentile Cost	0.00167254	1	4.796398	0.02852
☐	☐	Maximum Vorticity	0	1	0.109566	0.74064
☐	☐	Maximum TKE	0	1	0.279531	0.59701
☐	☑	Minimum Depth Requirement	-27.104862	1	69.82408	6.5e-17

Whole Model Test

Model	-LogLikelihood	DF	ChiSquare	Prob>ChiSq
Difference	142.17716	4	284.3543	<.0001*
Full	220.56319			
Reduced	362.74035			

RSquare (U)	0.3920
AICc	451.219
BIC	473.542
Observations (or Sum Wgts)	654

Measure	Training	Definition
Entropy RSquare	0.3920	1-Loglike(model)/Loglike(0)
Generalized RSquare	0.5261	(1-(L(0)/L(model))^(2/n))/(1-L(0)^(2/n))
Mean -Log p	0.3373	∑ -Log(ρ[j])/n
RMSE	0.3140	√ ∑(y[j]-ρ[j])²/n
Mean Abs Dev	0.1975	∑ |y[j]-ρ[j]|/n
Misclassification Rate	0.1208	∑ (ρ[j]≠ρMax)/n
N	654	n

Unit Odds Ratios

Per unit change in regressor

Term	Odds Ratio	Lower 95%	Upper 95%	Reciprocal
Maximum Velocity Ratio (25BL/s)	0.080206	0.012089	0.43773	12.467948
Maximum Velocity Ratio (10BL/s)	0.080447	0.026865	0.247497	12.430565
50th Percentile Cost	1.001674	1.000736	1.002655	0.9983289
Minimum Depth Requirement	1.69e-12	2.36e-14	9.27e-11	5.909e+11

(c) 50th percentile of cost

Figure A.2 (continued)

Current Estimates

Lock	Entered	Parameter	Estimate	nDF	Wald/Score ChiSq	"Sig Prob"
☑	☑	Intercept[0]	23.4131533	1	0	1
☐	☑	Maximum Velocity Ratio (25BL/s)	-2.1804936	1	3.543738	0.05977
☐	☑	Maximum Velocity Ratio (10BL/s)	-2.4689485	1	19.64115	0.00001
☐	☑	84th Percentile Cost	0.00113954	1	3.89891	0.04832
☐	☑	Maximum Vorticity	0.02792413	1	0.805735	0.36938
☐	☐	Maximum TKE	0	1	0.39356	0.53043
☐	☑	Minimum Depth Requirement	-25.027147	1	76.00239	2.8e-18

Whole Model Test

Model	-LogLikelihood	DF	ChiSquare	Prob>ChiSq
Difference	141.85692	5	283.7138	<.0001*
Full	220.88342			
Reduced	362.74035			

RSquare (U)	0.3911
AICc	453.897
BIC	480.665
Observations (or Sum Wgts)	654

Measure	Training	Definition
Entropy RSquare	0.3911	1-Loglike(model)/Loglike(0)
Generalized RSquare	0.5252	(1-(L(0)/L(model))^(2/n))/(1-L(0)^(2/n))
Mean -Log p	0.3377	∑ -Log(ρ[j])/n
RMSE	0.3136	√ ∑(y[j]-ρ[j])²/n
Mean Abs Dev	0.1975	∑ |y[j]-ρ[j]|/n
Misclassification Rate	0.1208	∑ (ρ[j]≠ρMax)/n
N	654	n

Unit Odds Ratios

Per unit change in regressor

Term	Odds Ratio	Lower 95%	Upper 95%	Reciprocal
Maximum Velocity Ratio (25BL/s)	0.112986	0.012465	0.8223	8.8506732
Maximum Velocity Ratio (10BL/s)	0.084674	0.028325	0.259599	11.81002
84th Percentile Cost	1.00114	1.000345	1.00195	0.9988611
Maximum Vorticity	1.028318	0.979336	1.079094	0.9724621
Minimum Depth Requirement	1.35e-11	1e-13	1.296e-9	7.399e+10

(d) 84th percentile of cost

Figure A.2 (continued)

Current Estimates

Lock	Entered	Parameter	Estimate	nDF	Wald/Score ChiSq	"Sig Prob"
☑	☑	Intercept[0]	23.709115	1	0	1
☐	☑	Maximum Velocity Ratio (25BL/s)	-2.1819198	1	4.275179	0.03867
☐	☑	Maximum Velocity Ratio (10BL/s)	-2.4028489	1	18.48585	1.71e-5
☐	☑	95th Percentile Cost	0.00112073	1	6.362683	0.01165
☐	☑	Maximum Vorticity	0.02695902	1	1.175312	0.27831
☐	☑	Minimum Depth Requirement	-25.572233	1	112.465	2.8e-26

Whole Model Test

Model	-LogLikelihood	DF	ChiSquare	Prob>ChiSq
Difference	141.09437	5	282.1887	<.0001*
Full	221.64598			
Reduced	362.74035			

RSquare (U)	0.3890
AICc	455.422
BIC	482.191
Observations (or Sum Wgts)	654

Measure	Training	Definition
Entropy RSquare	0.3890	1-Loglike(model)/Loglike(0)
Generalized RSquare	0.5229	(1-(L(0)/L(model))^(2/n))/(1-L(0)^(2/n))
Mean -Log p	0.3389	∑ -Log(ρ[j])/n
RMSE	0.3134	√ ∑(y[j]-ρ[j])²/n
Mean Abs Dev	0.1981	∑ |y[j]-ρ[j]|/n
Misclassification Rate	0.1208	∑ (ρ[j]≠ρMax)/n
N	654	n

Unit Odds Ratios

Per unit change in regressor

Term	Odds Ratio	Lower 95%	Upper 95%	Reciprocal
Maximum Velocity Ratio (25BL/s)	0.112825	0.012073	0.837232	8.8633048
Maximum Velocity Ratio (10BL/s)	0.09046	0.030273	0.27732	11.054624
95th Percentile Cost	1.001121	1.000252	1.002001	0.9988799
Maximum Vorticity	1.027326	0.977997	1.078443	0.9734011
Minimum Depth Requirement	7.84e-12	5.8e-14	7.5e-10	1.276e+11

(e) 95th percentile of cost

Figure A.2 (continued)

Current Estimates

Lock	Entered	Parameter	Estimate	nDF	Wald/Score ChiSq	"Sig Prob"
☑	☑	Intercept[0]	24.6693996	1	0	1
☐	☑	Depth/25	-27.267607	1	159.2931	1.6e-36
☐	☐	Depth/10	0	1	0.003515	0.95272

Whole Model Test

Model	-LogLikelihood	DF	ChiSquare	Prob>ChiSq
Difference	114.38377	1	228.7675	<.0001*
Full	248.35657			
Reduced	362.74035			

RSquare (U)	0.3153
AICc	500.732
BIC	509.679
Observations (or Sum Wgts)	654

Measure	Training	Definition
Entropy RSquare	0.3153	1-Loglike(model)/Loglike(0)
Generalized RSquare	0.4404	(1-(L(0)/L(model))^(2/n))/(1-L(0)^(2/n))
Mean -Log p	0.3798	∑ -Log(ρ[j])/n
RMSE	0.3320	√ ∑(y[j]-ρ[j])²/n
Mean Abs Dev	0.2257	∑ |y[j]-ρ[j]|/n
Misclassification Rate	0.1254	∑ (ρ[j]≠ρMax)/n
N	654	n

Unit Odds Ratios

Per unit change in regressor

Term	Odds Ratio	Lower 95%	Upper 95%	Reciprocal
Depth/25	1.44e-12	1.83e-14	8.82e-11	6.953e+11

Figure A.3: Preliminary combined variables across all WWP structures selected by stepwise forward regression and their inclusion in logistic regression.

Current Estimates

Lock	Entered	Parameter	Estimate	nDF	Wald/Score ChiSq	"Sig Prob"
☑	☑	Intercept[0]	45.0054647	1	0	1
☐	☑	Depth/25	-49.734777	1	66.64512	3.3e-16
☐	☐	Depth/10	0	1	0.614401	0.43314

Whole Model Test

Model	-LogLikelihood	DF	ChiSquare	Prob>ChiSq
Difference	52.19046	1	104.3809	<.0001*
Full	65.70558			
Reduced	117.89605			

RSquare (U)	0.4427
AICc	135.471
BIC	142.047
Observations (or Sum Wgts)	204

Measure	Training	Definition
Entropy RSquare	0.4427	1-Loglike(model)/Loglike(0)
Generalized RSquare	0.5845	(1-(L(0)/L(model))^(2/n))/(1-L(0)^(2/n))
Mean -Log p	0.3221	∑ -Log(ρ[j])/n
RMSE	0.2932	√ ∑(y[j]-ρ[j])²/n
Mean Abs Dev	0.1769	∑ |y[j]-ρ[j]|/n
Misclassification Rate	0.0931	∑ (ρ[j]≠ρMax)/n
N	204	n

Unit Odds Ratios

Per unit change in regressor

Term	Odds Ratio	Lower 95%	Upper 95%	Reciprocal
Depth/25	2.51e-22	8.22e-28	1.94e-17	3.977e+21

(a) WWP1

Figure A.4: Preliminary combined variables for each WWP structure selected by stepwise forward regression and their inclusion in logistic regression for: (a) WWP1, (b) WWP2, and (c) WWP3.

Current Estimates

Lock	Entered	Parameter	Estimate	nDF	Wald/Score ChiSq	"Sig Prob"
☑	☑	Intercept[0]	24.8875464	1	0	1
☐	☑	Depth/25	-27.001636	1	50.01188	1.5e-12
☐	☐	Depth/10	0	1	5.612e-5	0.99402

Whole Model Test

Model	-LogLikelihood	DF	ChiSquare	Prob>ChiSq
Difference	40.15399	1	80.30798	<.0001*
Full	69.95653			
Reduced	110.11052			

RSquare (U)	0.3647
AICc	143.977
BIC	150.428
Observations (or Sum Wgts)	192

Measure	Training	Definition
Entropy RSquare	0.3647	1-Loglike(model)/Loglike(0)
Generalized RSquare	0.5009	(1-(L(0)/L(model))^(2/n))/(1-L(0)^(2/n))
Mean -Log p	0.3644	∑ -Log(ρ[j])/n
RMSE	0.3256	√ ∑(y[j]-ρ[j])²/n
Mean Abs Dev	0.2120	∑ |y[j]-ρ[j]|/n
Misclassification Rate	0.1250	∑ (ρ[j]≠ρMax)/n
N	192	n

Unit Odds Ratios

Per unit change in regressor

Term	Odds Ratio	Lower 95%	Upper 95%	Reciprocal
Depth/25	1.88e-12	6.17e-16	1.912e-9	5.329e+11

(b) WWP2

Figure A.4 (continued)

Current Estimates

Lock	Entered	Parameter	Estimate	nDF	Wald/Score ChiSq	"Sig Prob"
☑	☑	Intercept[0]	20.4208682	1	0	1
☐	☐	Depth/10	0	0	0	.
☐	☑	Depth/25	-22.610631	1	54.96304	1.2e-13

Whole Model Test

Model	-LogLikelihood	DF	ChiSquare	Prob>ChiSq
Difference	35.85367	1	71.70733	<.0001*
Full	97.82577			
Reduced	133.67943			

RSquare (U)	0.2682
AICc	199.699
BIC	206.757
Observations (or Sum Wgts)	258

Measure	Training	Definition
Entropy RSquare	0.2682	1-Loglike(model)/Loglike(0)
Generalized RSquare	0.3761	(1-(L(0)/L(model))^(2/n))/(1-L(0)^(2/n))
Mean -Log p	0.3792	∑ -Log(ρ[j])/n
RMSE	0.3371	√ ∑(y[j]-ρ[j])²/n
Mean Abs Dev	0.2271	∑ |y[j]-ρ[j]|/n
Misclassification Rate	0.1434	∑ (ρ[j]≠ρMax)/n
N	258	n

Unit Odds Ratios

Per unit change in regressor

Term	Odds Ratio	Lower 95%	Upper 95%	Reciprocal
Depth/25	1.51e-10	3.09e-13	4.96e-8	6.602e+9

(c) WPP3

Figure A.4 (continued)

LIST OF ABBREVIATIONS

3-D	three-dimensional
AIC	Akaike Information Criterion
CFD	computational fluid dynamics models
CPW	Colorado Parks and Wildlife
CWCB	Colorado Water Conservation Board
CWI	Colorado Water Institute
IPOS	intensity, periodicity, orientation, and scale
NOAA	National Oceanic and Atmospheric Administration
pers. comm.	personal communication
PIT	passive integrated transponder
®	registered
RANS	Reynolds-Averaged Navier-Stokes
RNG	renormalization group
TKE	turbulent kinetic energy
TI	turbulent intensity
USA	United States of America
USGS	U. S. Geological Survey
VOF	volume of fluid
WWP	whitewater park
WWP1	whitewater park 1
WWP2	whitewater park 2
WWP3	whitewater park 3